

¹ **Title:** Carbon cycling in mature and regrowth forests globally: a macroecological synthesis based on the
² Global Forest Carbon (ForC) database

³ **Authors:**

⁴ Kristina J. Anderson-Teixeira^{1,2*}

⁵ Valentine Herrmann¹

⁶ Becky Banbury Morgan^{1,3}

⁷ Ben Bond-Lamberty⁴

⁸ Susan C. Cook-Patton⁵

⁹ Abigail E. Ferson^{1,6}

¹⁰ Helene C. Muller-Landau²

¹¹ Maria M. H. Wang^{1,7}

¹² **Author Affiliations:**

¹³ 1. Conservation Ecology Center; Smithsonian Conservation Biology Institute; National Zoological Park,
¹⁴ Front Royal, VA 22630, USA

¹⁵ 2. Center for Tropical Forest Science-Forest Global Earth Observatory; Smithsonian Tropical Research
¹⁶ Institute; Panama, Republic of Panama

¹⁷ 3. School of Geography, University of Leeds, Leeds, UK

¹⁸ 4. Joint Global Change Research Institute, Pacific Northwest National Laboratory, College Park
¹⁹ Maryland 20740, USA

²⁰ 5. The Nature Conservancy; Arlington VA 22203, USA

²¹ 6. College of Natural Resources, University of Idaho; Moscow, Idaho 83843, USA

²² 7. Grantham Centre for Sustainable Futures and Department of Animal and Plant Sciences, University of
²³ Sheffield, Western Bank, Sheffield, South Yorkshire S10 2TN, UK

²⁴ *corresponding author: teixeirak@si.edu; +1 540 635 6546

²⁵ **Summary**

²⁶ *Background.* Earth's climate is closely linked to forests, which strongly influence atmospheric carbon dioxide
²⁷ (CO_2) and climate by their impact on the global carbon (C) cycle. However, efforts to incorporate forests
²⁸ into climate models and CO_2 accounting frameworks have been constrained by a lack of accessible,
²⁹ global-scale data on how C cycling varies across forest types and stand ages.

³⁰ *Methods/Design.* Here, we draw from the Global Forest Carbon Database, *ForC*, to provide a macroscopic
³¹ overview of C cycling in the world's forests, giving special attention to stand age-related variation.

³² Specifically, we use 11923 *ForC* records from 865 geographic locations representing 34 C cycle variables to
³³ characterize ensemble C budgets for four broad forest types (tropical broadleaf evergreen, temperate
³⁴ broadleaf, temperate conifer, and taiga), including estimates for both mature and regrowth (age <100 years)
³⁵ forests. For regrowth forests, we quantify age trends for all variables with sufficient data.

³⁶ *Review Results/ Synthesis.* *ForC v3.0* yielded a comprehensive picture of C cycling in the world's major
³⁷ forest biomes. The rate of C cycling generally increased from boreal to tropical regions in both mature and
³⁸ regrowth forests, whereas C stocks showed less directional variation. The majority of flux variables, together
³⁹ with most live biomass pools, increased significantly with stand age. Importantly, there was generally good
⁴⁰ closure of C budgets, *i.e.*, internal consistency in the *ForC* data.

⁴¹ *Discussion.* As climate change accelerates, understanding and managing the carbon dynamics of forests is
⁴² critical to forecasting, mitigation, and adaptation. This synthetic and internally consistent global overview of
⁴³ C stocks and fluxes across biomes and stand ages will help to advance these efforts.

⁴⁴ *Key words:* forest ecosystems; carbon cycle; stand age; productivity; respiration; biomass; global

45 **Background**

46 Forest ecosystems are shaping the course of climate change through their influence on atmospheric carbon
47 dioxide (CO₂; Bonan 2008, Friedlingstein *et al* 2019, IPCC 2018). Despite the centrality of forest C cycling
48 in regulating atmospheric CO₂, important uncertainties in climate models (Friedlingstein *et al* 2006, Krause
49 *et al* 2018, Bonan *et al* 2019, Di Vittorio *et al* 2020) and CO₂ accounting frameworks (Pan *et al* 2011) can be
50 traced to lack of accessible, comprehensive data on how C cycling varies across forest types and in relation to
51 stand history. These require large-scale databases with global coverage, which runs contrary to the nature in
52 which forest C stocks and fluxes are measured and published. While remote sensing measurements are
53 increasingly useful for global- or regional-scale estimates of a few critical variables (e.g., aboveground
54 biomass: Hu *et al* 2016, Spawn *et al* 2020, gross primary productivity, *GPP*: Li and Xiao 2019, Saatchi *et al*
55 2011), measurement and validation of most forest C stocks and fluxes require intensive on-the-ground data
56 collection.

57 A robust understanding of forest impacts on global C cycling is essential. Annual gross CO₂ sequestration in
58 forests (gross primary productivity, *GPP*) is estimated at >69 Gt C yr⁻¹ (Badgley *et al* 2019), or >7 times
59 average annual fossil fuel emissions from 2009-2018 (9.5 ± 0.5 Gt C yr⁻¹; Friedlingstein *et al* 2019). Most of
60 this enormous C sequestration is counterbalanced by CO₂ releases to the atmosphere through ecosystem
61 respiration (R_{eco}) or fire, with forests globally dominant as sources of both soil respiration (Warner *et al*
62 2019) and fire emissions (Werf *et al* 2017). In recent years, the remaining CO₂ sink averaged 3.2 ± 0.6 GtC
63 yr⁻¹ from 2009-2018, offsetting 29% of anthropogenic fossil fuel emissions (Friedlingstein *et al* 2019). Yet, this
64 sink is reduced by deforestation, estimated at ~1 Gt C yr⁻¹ in recent decades (Pan *et al* 2011, Tubiello *et al*
65 2020), reducing the net forest sink to ~1.1-2.2 Gt C yr⁻¹ across Earth's forests (Friedlingstein *et al* 2019).

66 The future of the current forest C sink is dependent both upon forest responses to climate change itself and
67 human land use decisions, which will feedback and strongly influence the course of climate change.

68 Regrowing forests in particular will play an important role (Pugh *et al* 2019), as almost two-thirds of the
69 world's forests were secondary as of 2010 (FAO 2010). As anthropogenic and climate-driven disturbances
70 impact an growing proportion of Earth's forests (Andela *et al* 2017, McDowell *et al* 2020), understanding the
71 carbon dynamics of regrowth forests is increasingly important (Anderson-Teixeira *et al* 2013). Although age
72 trends in aboveground biomass have been relatively well-studied and synthesized globally (Cook-Patton *et al*
73 2020), a relative dearth of data and synthesis on other C stocks and fluxes in secondary forests points to an
74 under-filled need to characterize age-related trends in forest C cycling. Such understanding is particularly
75 critical for reducing uncertainty regarding the potential for carbon uptake and climate change mitigation by
76 regrowth forests (Krause *et al* 2018, Cook-Patton *et al* 2020). Understanding, modeling, and managing
77 forest-atmosphere CO₂ exchange is thus central to efforts to mitigate climate change (Grassi *et al* 2017,
78 Griscom *et al* 2017, Cavaleri *et al* 2015).

79 Despite the importance of forests, comprehensive global studies have historically been limited by the
80 scattered and more local nature of research studies. Primary research articles typically cover only a small
81 numbers of sites at a time. The rare exceptions that span regions or continents with rare exceptions spanning
82 regions or continents are typically coordinated through research networks such as ForestGEO
83 (Anderson-Teixeira *et al* 2015, e.g., Lutz *et al* 2018), NEON (Schimel *et al* 2007), or FLUXNET (Baldocchi
84 *et al* 2001, e.g., Novick *et al* 2018). The result of decades of research on forest C cycling is that tens of
85 thousands of records have been distributed across literally thousands of scientific articles –often behind
86 paywalls– along with variation in data formats, units, measurement methods, *etc.* In this format, the data

87 are effectively inaccessible for many global-scale analyses, including those attempting to benchmark model
88 performance with global data (Clark et al 2017, Luo et al 2012), quantify the role of forests in the global
89 C cycle (e.g., Pan *et al* 2011), or use book-keeping methods to quantify actual or scenario-based exchanges of
90 CO₂ between forests and the atmosphere (Griscom *et al* 2017, Houghton 2020).

91 To address the need for global-scale analyses of forest C cycling, we recently developed *ForC*
92 (Anderson-Teixeira *et al* 2016, 2018). *ForC* contains published estimates of forest ecosystem C stocks and
93 annual fluxes (>50 variables), with the different variables capturing the unique ecosystem pools (e.g., woody,
94 foliage, and root biomass; dead wood) and flux types (e.g, gross and net primary productivity; soil, root, and
95 ecosystem respiration). These data are ground-based measurements, and *ForC* contains associated data
96 required for interpretation (e.g., stand history, measurement methods). Data have been amalgamated from
97 original peer-reviewed publications, either directly or via intermediary data compilations. Since its most
98 recent publication (Anderson-Teixeira *et al* 2018), *ForC* has grown to include two additional large databases:
99 the Global Soil Respiration Database (SRDB; Bond-Lamberty and Thomson 2010) and the Global
100 Reforestation Opportunity Assessment database (GROA; Cook-Patton *et al* 2020) that also synthesized
101 published forest C data. Following these additions, *ForC* currently contains 39762 records from 10608 plots
102 and 1532 distinct geographic areas representing all forested biogeographic and climate zones. This represents
103 an 129% increase in records from the prior publication (Anderson-Teixeira *et al* 2018).

104 Here, we provide a robust and comprehensive analysis of carbon cycling from a stand to global level, and by
105 biome and stand age, using the largest global compilation of forest carbon data, which is available in our
106 open source Global Carbon Forest database (*ForC*; Fig. 1). Our primary goal is to provide a data-driven
107 summary of our current state of knowledge on broad trends in forest C cycling. Specifically, we address three
108 broad questions:

- 109 1. How thoroughly can we represent C budgets for each of the world's major forest biomes (*i.e.*, tropical,
110 temperate broadleaf and deciduous, boreal) based on the current *ForC* data?
- 111 2. How do C cycling vary across the world's major forest biomes?
- 112 3. How does C cycling vary with stand age (in interaction with biome)?

113 While components of these questions have been previously addressed (Luyssaert *et al* 2007,
114 Anderson-Teixeira *et al* 2016, Cook-Patton *et al* 2020, Banbury Morgan *et al* n.d.), our analysis represents
115 by far the most comprehensive analysis of C cycling in global forests, and will serve as a foundation for
116 improved understanding of global forest C cycling and highlight where key sources of uncertainty still reside.

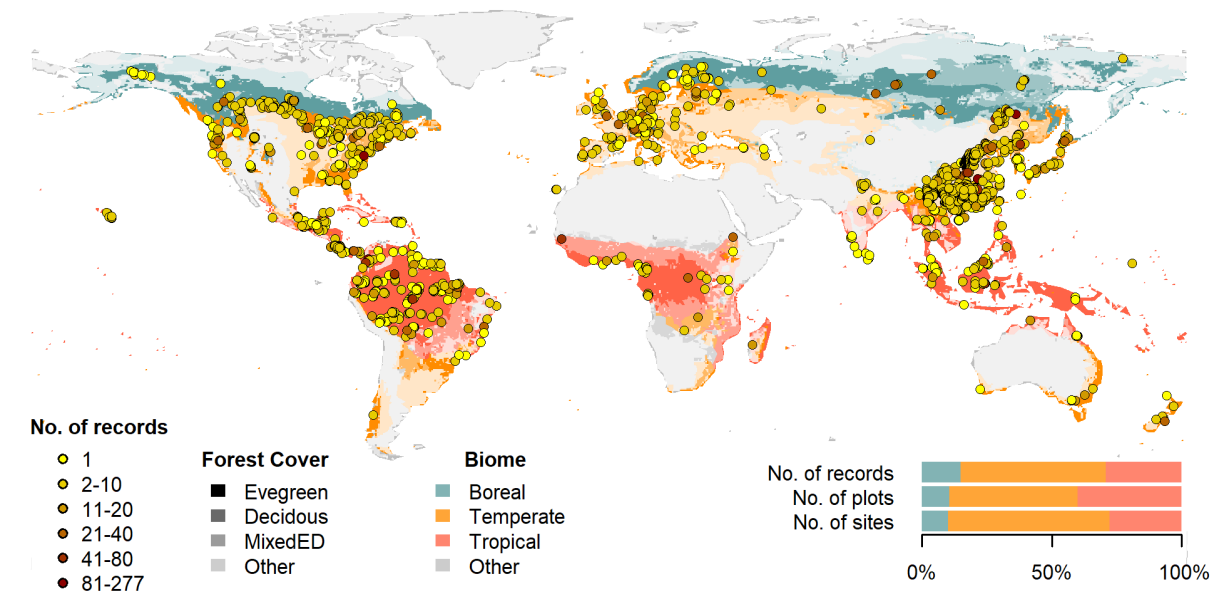


Figure 1 | Map of sites included in this analysis. Symbols are colored according to the number of records at each site. Underlying map shows coverage of evergreen, deciduous, and mixed forests (from SYNMAP; Jung et al. 2006) and biomes. Distribution of sites, plots, and records among biomes is shown in the inset.

117 Methods/ Design

118 This review synthesizes data from the *ForC* database (Fig. 1; <https://github.com/forc-db/ForC>;
 119 Anderson-Teixeira *et al* 2016, 2018). *ForC* amalgamates numerous intermediary data sets (*e.g.*, Luyssaert *et*
 120 *al* 2007, Bond-Lamberty and Thomson 2010, Cook-Patton *et al* 2020) and original studies. Original
 121 publications were referenced to check values and obtain information not contained in intermediary data sets,
 122 although this process has not been completed for all records. The database was developed with goals of
 123 understanding how C cycling in forests varies across broad geographic scales and as a function of stand age.
 124 As such, there has been a focus on incorporating data from regrowth forests (*e.g.*, Anderson *et al* 2006,
 125 Martin *et al* 2013, Bonner *et al* 2013) and obtaining stand age data when possible (83% of records in v.2.0;
 126 Anderson-Teixeira *et al* 2018). Particular attention was given to developing the database for tropical forests
 127 (Anderson-Teixeira *et al* 2016), which represented roughly one-third of records in *ForC* v2.0
 128 (Anderson-Teixeira *et al* 2018). Since publication of *ForC* v2.0, we added the following data to *ForC*: the
 129 Global Database of Soil Respiration Database (*SRDB* v4, 9488 records; Bond-Lamberty and Thomson 2010),
 130 the Global Reforestation Opportunity Assessment database (*GROA* v1.0, 10116 records; Cook-Patton *et al*
 131 2020, Anderson-Teixeira *et al* 2020). We have also added data from individual publications, with a particular
 132 focus on productivity (*e.g.*, Taylor *et al* 2017), dead wood, and ForestGEO sites (*e.g.*, Lutz *et al* 2018, p
 133 @johnson_climate_2018). The database version used for this analysis has been tagged as a new release on
 134 Github (v3.0) and assigned a DOI through Zenodo (DOI: TBD).
 135 To facilitate analyses, we created a simplified version of *ForC*, *ForC-simplified*
 136 (https://github.com/forc-db/ForC/blob/master/ForC_simplified), which we analyzed here. In generating

137 *ForC-simplified*, all measurements originally expressed in units of dry organic matter (OM) were converted
138 to units of C using the IPCC default of $C = 0.47 * OM$ (IPCC 2018). Duplicate or otherwise conflicting
139 records were reconciled as described in Appendix S1, resulting in a total of 22265 records (56% size of total
140 database). Records were filtered to remove plots that had undergone significant anthropogenic management
141 or major disturbance since the most recent stand initiation event. Specifically, we removed all plots flagged
142 as managed in ForC-simplified (13.9%). This included plots with any record of managements manipulating
143 CO_2 , temperature, hydrology, nutrients, or biota, as well as any plots whose site or plot name contained the
144 terms “plantation”, “planted”, “managed”, “irrigated”, or “fertilized”. Plots flagged as disturbed in
145 ForC-simplified (5.6%) included stands that had undergone any notable anthropogenic thinning or partial
146 harvest. We retained sites that were grazed or had undergone low severity natural disturbances (<10%
147 mortality) including droughts, major storms, fires, and floods. We removed all plots for which no stand
148 history information had been retrieved (5.7%). In total, this resulted in 17349 records (43.6% of the records
149 in the database) being eligible for inclusion in the analysis.

150 We selected 23 annual flux and 11 C stock variables for inclusion in the analysis (Table 1). These different
151 flux and stock variables represent different pools (e.g., aboveground biomass, root biomass, dead wood) and
152 levels of combination (e.g., total net primary productivity, NPP , versus the individual elements of NPP
153 such as foliage, roots, and branches). Note that two flux variables, aboveground heterotrophic (R_{het-ag}) and
154 total (R_{het}) respiration, were included for conceptual completeness but had no records in *ForC* (Table 1).
155 Records for our focal variables represented 90.3% of the total records eligible for inclusion. For this analysis,
156 we combined some of ForC’s specific variables into more broadly defined variables. Specifically, net ecosystem
157 exchange (measured by eddy-covariance; Baldocchi *et al* 2001) and biometric estimates of NEP were
158 combined into the single variable NEP (Table 1). Furthermore, for NPP , aboveground NPP ($ANPP$),
159 and the litterfall component of $ANPP$ ($ANPP_{litterfall}$), *ForC* variables specifying inclusion of different
160 components were combined (e.g., measurements including or excluding fruit and flower production and
161 herbivory). Throughout ForC, for all measurements drawing from tree census data (e.g., biomass,
162 productivity), the minimum diameter breast height (DBH) threshold for tree census was $\leq 10\text{cm}$. All records
163 were measured directly or derived from field measurements (as opposed to modeled).

164 We grouped forests into four broad biome types based on climate zones and dominant vegetation type
165 (tropical broadleaf, temperate broadleaf, temperate needleleaf, and boreal needleleaf) and two age
166 classifications (young and mature). Climate zones (Fig. 1) were defined based on site geographic coordinates
167 according to Köppen-Geiger zones (Rubel and Kottek 2010). We defined the tropical biome as including all
168 equatorial (A) zones, temperate biomes as including all warm temperate (C) zones and warmer snow
169 climates (Dsa, Dsb, Dwa, Dwb, Dfa, and Dfb), and the boreal biome as including the colder snow climates
170 (Dsc, Dsd, Dwc, Dwd, Dfc, and Dfd). Any forests in dry (B) and polar (E) Köppen-Geiger zones were
171 excluded from the analysis. We defined leaf type (broadleaf / needleleaf) was based on descriptions in
172 original publications (prioritized) or values extracted from a global map based on satellite observations
173 (SYNMAP; Jung *et al* 2006). For young tropical forests imported from *GROA* but not yet classified by leaf
174 type, we assumed that all were broadleaf, consistent with the rarity of naturally regenerating needleleaf
175 forests in the tropics. We also classified forests as “young” (< 100 years) or “mature” (≥ 100 years or
176 classified as “mature”, “old growth”, “intact”, or “undisturbed” in original publication). Assigning stands to
177 these groupings required the exclusion of records for which *ForC* lacked geographic coordinates (0.4% of sites
178 in full database) or records of stand age (5.7% of records in full database). We also excluded records of stand

Table 1. Carbon cycle variables included in this analysis, their sample sizes, and summary of biome differences and age trends.

Variable	Description	N records			biome differences*	age trend†
		records	plots	geographic areas		
Annual fluxes						
<i>NEP</i>	net ecosystem production or net ecosystem exchange (+ indicates C sink)	329	146	88	n.s.	+; xB
<i>GPP</i>	gross primary production ($NPP + R_{auto}$ or $R_{eco} - NEE$)	303	115	84	TrB > TeB \geq TeN \geq BoN	+; xB
<i>NPP</i>	net primary production ($ANPP + BNPP$)	214	112	74	TrB > TeB \geq TeN $>$ BoN	n.s.
<i>ANPP</i>	aboveground <i>NPP</i>	343	236	131	TrB > TeB \geq TeN $>$ BoN	+; xB
<i>ANPP_{woody}</i>	woody production ($ANPP_{stem} + ANPP_{branch}$)	64	53	37	n.s.	+
<i>ANPP_{stem}</i>	woody stem production	217	190	117	TrB > TeN \geq TeB \geq BoN	n.s.
<i>ANPP_{branch}</i>	branch turnover	69	59	42	TrB > TeB \geq TeN	n.s.
<i>ANPP_{foliage}</i>	foliage production, typically estimated as annual leaf litterfall	162	132	88	TrB > TeB \geq TeN $>$ BoN	+
<i>ANPP_{litterfall}</i>	litterfall, including leaves, reproductive structures, twigs, and sometimes branches	82	70	55	n.s.	+
<i>ANPP_{repro}</i>	production of reproductive structures (flowers, fruits, seeds)	51	44	34	n.t.	n.t.
<i>ANPP_{folivory}</i>	foliar biomass consumed by folivores	20	12	11	n.t.	n.t.
<i>M_{woody}</i>	woody mortality—i.e., B_{ag} of trees that die	18	18	18	n.t.	n.t.
<i>BNPP</i>	belowground NPP ($BNPP_{coarse} + BNPP_{fine}$)	148	116	79	TrB > TeN \geq TeB \geq BoN	+
<i>BNPP_{coarse}</i>	coarse root production	77	56	36	TeN \geq TrB	n.s.
<i>BNPP_{fine}</i>	fine root production	123	99	66	n.s.	+
<i>R_{eco}</i>	ecosystem respiration ($R_{auto} + R_{het}$)	213	98	70	TrB > TeB \geq TeN	+
<i>R_{auto}</i>	autotrophic respiration ($(R_{auto-ag} + R_{root})$)	24	23	15	n.t.	n.t.
<i>R_{auto-ag}</i>	aboveground autotrophic respiration (i.e., leaves and stems)	2	2	1	n.t.	n.t.
<i>R_{root}</i>	root respiration	181	139	95	TrB \geq TeB	+
<i>R_{soil}</i>	soil respiration ($(R_{het-soil} + R_{root})$)	627	411	229	TrB > TeB $>$ TeN \geq BoN	n.s.
<i>R_{het-soil}</i>	soil heterotrophic respiration	197	156	100	TrB > TeB \geq TeN	n.s.
<i>R_{het-ag}</i>	aboveground heterotrophic respiration	0	0	0	-	-
<i>R_{het}</i>	heterotrophic respiration ($(R_{het-ag} + R_{het-soil})$)	0	0	0	-	-
Stocks						
<i>B_{tot}</i>	total live biomass ($B_{ag} + B_{root}$)	188	157	87	TrB \geq TeB $>$ BoN	+; xB
<i>B_{ag}</i>	aboveground live biomass ($B_{ag-wood} + B_{foliage}$)	4466	4072	621	TrB \geq TeN \geq TeB $>$ BoN	+; xB
<i>B_{ag-wood}</i>	woody component of aboveground biomass	115	102	64	TeN $>$ TrB \geq BoN	+; xB
<i>B_{foliage}</i>	foliage biomass	134	115	72	TeN $>$ TrB \geq BoN \geq TeB	+; xB
<i>B_{root}</i>	total root biomass ($B_{root-coarse} + B_{root-fine}$)	2329	2298	360	n.s.	+; xB
<i>B_{root-coarse}</i>	coarse root biomass	134	120	73	TeN $>$ TeB \geq BoN	+; xB
<i>B_{root-fine}</i>	fine root biomass	226	180	109	n.s.	+; xB
<i>DW_{tot}</i>	deadwood ($DW_{standing} + DW_{down}$)	79	73	42	n.t.	+; xB
<i>DW_{standing}</i>	standing dead wood	36	35	22	n.t.	n.t.
<i>DW_{down}</i>	fallen dead wood, including coarse and sometimes fine woody debris	278	265	37	n.t.	+; xB
<i>OL</i>	organic layer / litter/ forest floor	474	413	115	n.s.	+; xB

* Tr: Tropical, TeB: Temperate Broadleaf, TeN: Temperate Needleleaf, B: Boreal, n.s.: no significant differences, n.t.: not tested

† + or -: significant positive or negative trend, xB: significant age x biome interaction, n.s.: no significant age trend, n.t.: not tested

179 age = 0 year (0.8% of records in full database). In total, our analysis retained 76.1 of the focal variable

180 records for forests of known age. Numbers of records by biome and age class are given in Table S1.

181 Data were summarized to produce schematics of C cycling across the eight biome by age group combinations
182 identified above. To obtain the values reported in the C cycle schematics, we first averaged any repeated
183 measurements within a plot. Values were then averaged across geographically distinct areas, defined as plots
184 clustered within 25 km of one another (*sensu* Anderson-Teixeira *et al* 2018), weighting by area sampled if
185 available for all records. This step was taken to avoid pseudo-replication.

186 We tested whether the C budgets described above “closed”—*i.e.*, whether they were internally consistent.
187 Specifically, we first defined relationships among variables: for example, $NEP = GPP - R_{eco}$,
188 $BNPP = BNPP_{coarse} + BNPP_{fine}$, $DW_{tot} = DW_{standing} + DW_{down}$). Henceforth, we refer to the
189 variables on the left side of the equation as “aggregate” fluxes or stocks, and those that are summed as
190 “component” fluxes or stocks, noting that the same variable can take both aggregate and component positions
191 in different relationships. We considered the C budget for a given relationship “closed” when component
192 variables summed to within one standard deviation of the aggregate variable.

193 To test for differences across mature forest biomes, we also examined how stand age impacted fluxes and
194 stocks, employing a mixed effects model (“lmer” function in “lme4” R package; Bates *et al* 2015) with biome
195 as fixed effect and plot nested within geographic.area as random effects on the intercept. When Biome had a
196 significant effect, we looked at a Tukey’s pairwise comparison to see which biomes were significantly different
197 from one another. This analysis was run for variables with records for at least seven distinct geographic areas
198 in more than one biome, excluding any biomes that failed this criteria (Table 1).

199 To test for age trends in young (<100yrs) forests, we employed a mixed effects model with biome and
200 $\log_{10}[\text{stand.age}]$ as fixed effects and plot nested within geographic.area as a random effect on the intercept.
201 This analysis was run for variables with records for at least three distinct geographic areas in more than one
202 biome, excluding any biomes that failed this criteria (Table 1). When the effect of stand age was significant
203 at $p \leq 0.05$ and when each biome had records for stands of at least 10 different ages, a biome \times stand.age
204 interaction was included in the model.

205 To facilitate the accessibility of our results and data, and to allow for rapid updates as additional data
206 become available, we have automated all database manipulation, analyses, and figure production in R (R
207 Core Team 2020).

208 Review Results/ Synthesis

209 Data Coverage

210 Of the 39762 records in *ForC* v3.0, 11923 met our strict criteria for inclusion in this study (Fig. 1). These
211 records were distributed across 5062 plots in 865 distinct geographic areas. Of the 23 flux and 11 stock
212 variables mapped in these diagrams, *ForC* contained sufficient mature forest data for inclusion in our
213 statistical analyses (*i.e.*, records from ≥ 7 distinct geographic areas) for 20 fluxes and 9 stocks in tropical
214 broadleaf forests, 15 fluxes and 8 stocks in temperate broadleaf forests, 14 fluxes and 7 stocks in temperate
215 conifer forests, and 8 fluxes and 7 stocks in boreal forests. For regrowth forests (<100 yrs), *ForC* contained
216 sufficient data for inclusion in our statistical analyses (*i.e.*, records from ≥ 3 distinct geographic areas) for 11
217 fluxes and 10 stocks in tropical broadleaf forests, 16 fluxes and 10 stocks in temperate broadleaf forests, 16
218 fluxes and 10 stocks in temperate conifer forests, and 14 fluxes and 9 stocks in boreal forests.

219 **C cycling in mature forests**

220 Average C cycles for mature tropical broadleaf, temperate broadleaf, temperate conifer, and boreal forests \geq
221 100 years old and with no known major natural or anthropogenic disturbance are presented in Figures 2-5
222 (and available in tabular format in the *ForC* release accompanying this publication:
223 [ForC/numbers_and_facts/ForC_variable_averages_per_Biome.csv](#)).

224 For variables with records from ≥ 7 distinct geographic areas, these ensemble C budgets were generally
225 consistent. That is, component variables summed to within one standard deviation of their respective
226 aggregate variables in all but one instance. In the temperate conifer biome, the average composite measure of
227 root biomass (B_{root}) was less than the combined average value of coarse and fine root biomass ($B_{root-coarse}$
228 and $B_{root-fine}$, respectively). This lack of closure was driven by very high estimates of $B_{root-coarse}$ from
229 high-biomass forests of the US Pacific Northwest.

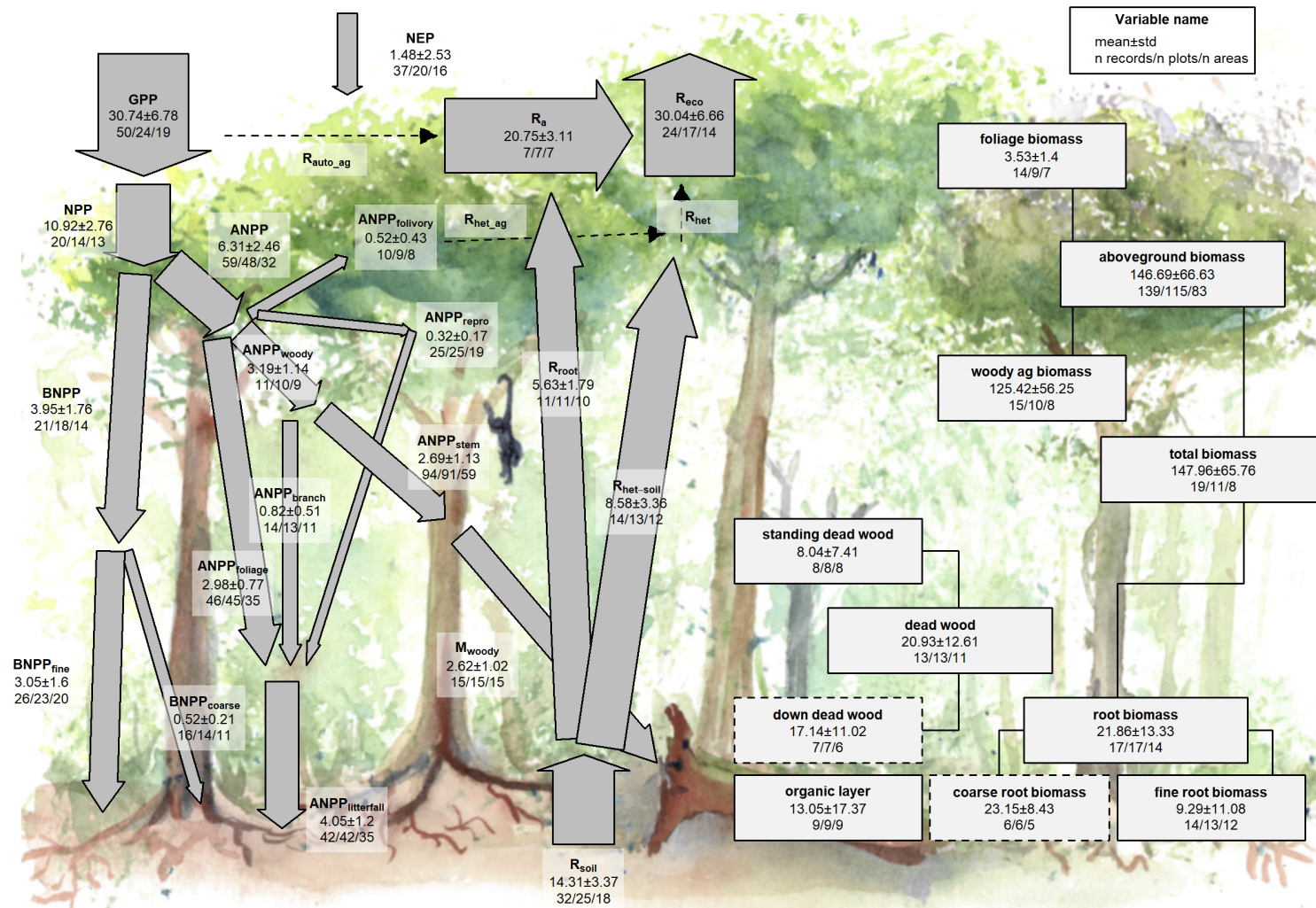


Figure 2 | C cycle diagram for mature tropical broadleaf forests. Arrows indicate fluxes ($\text{Mg C ha}^{-1} \text{ yr}^{-1}$); boxes indicate stocks (Mg C ha^{-1}), with variables as defined in Table 1. Presented are mean \pm std, where geographically distinct areas are treated as the unit of replication. Dashed shape outlines indicate variables with records from <7 distinct geographic areas, and dashed arrows indicate fluxes with no data. To illustrate the magnitude of different fluxes, arrow size is proportional to the square root of corresponding flux. Asterisk after variable name indicates lack of C cycle closure.

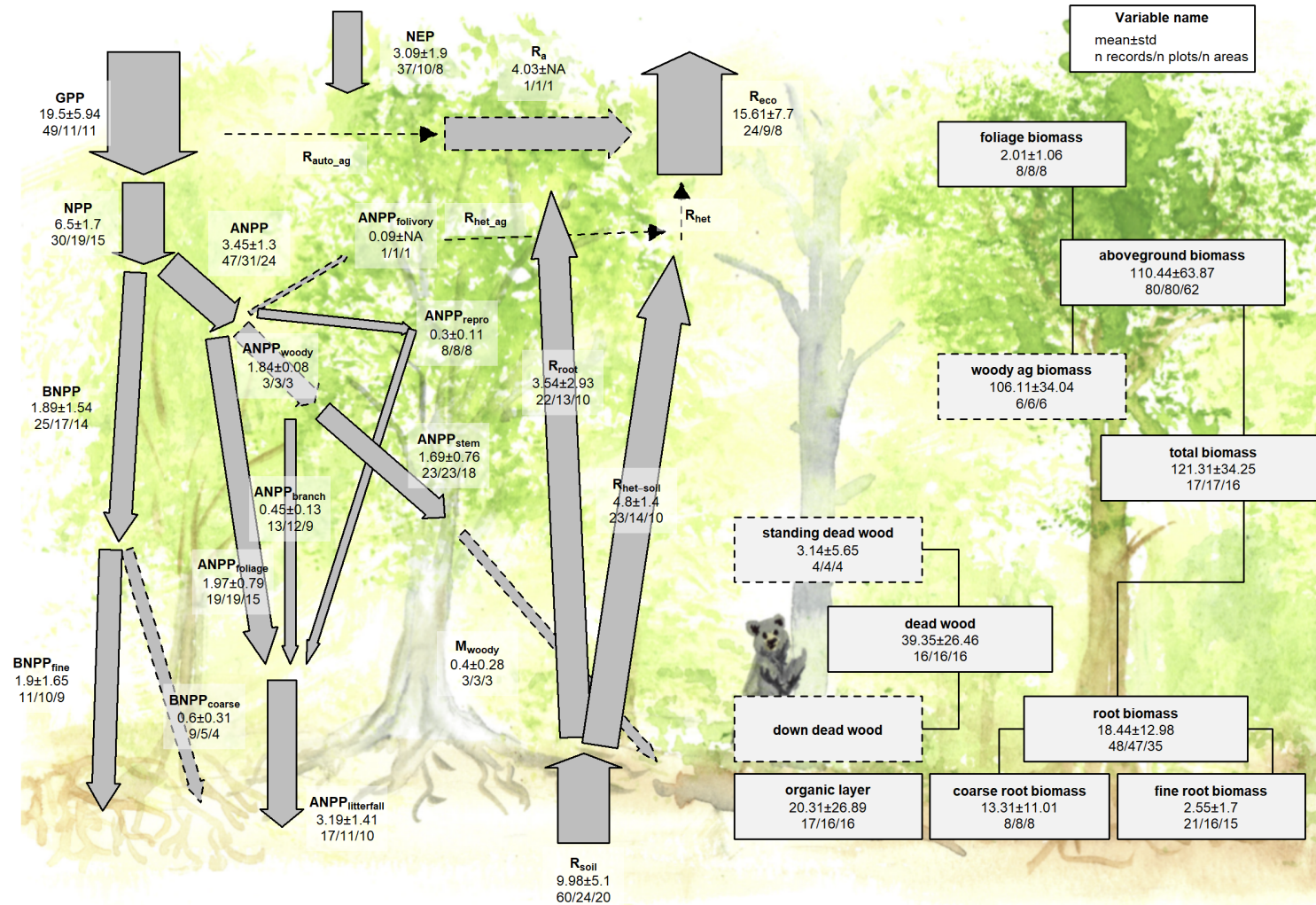


Figure 3 | C cycle diagram for mature temperate broadleaf forests. Arrows indicate fluxes ($Mg\ C\ ha^{-1}\ yr^{-1}$); boxes indicate stocks ($Mg\ C\ ha^{-1}$), with variables as defined in Table 1. Presented are mean \pm std, where geographically distinct areas are treated as the unit of replication. Dashed shape outlines indicate variables with records from <7 distinct geographic areas, and dashed arrows indicate fluxes with no data. To illustrate the magnitude of different fluxes, arrow size is proportional to the square root of corresponding flux. Asterisk after variable name indicates lack of C cycle closure.

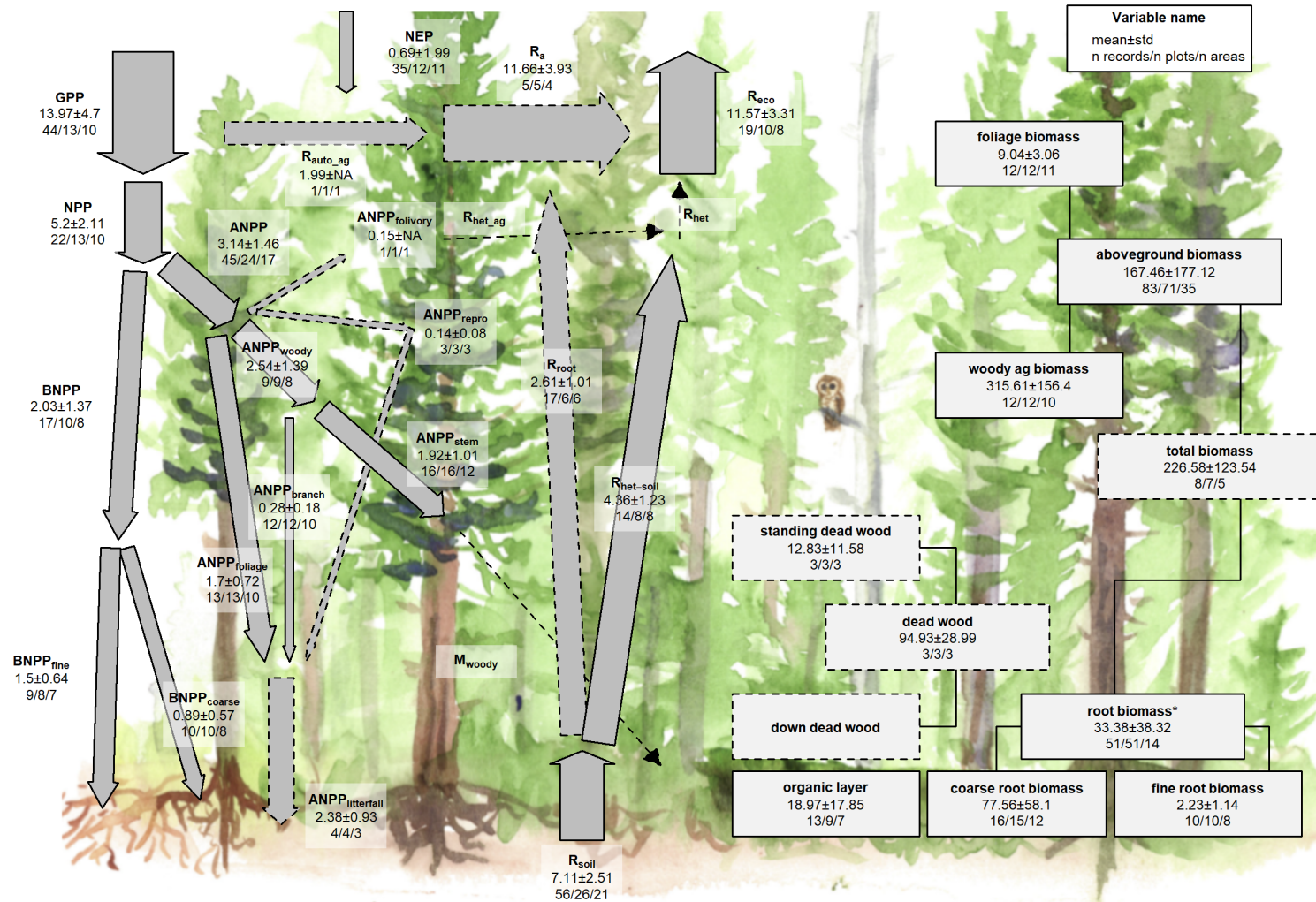


Figure 4 | C cycle diagram for mature temperate conifer forests. Arrows indicate fluxes ($\text{Mg C ha}^{-1} \text{ yr}^{-1}$); boxes indicate stocks (Mg C ha^{-1}), with variables as defined in Table 1. Presented are mean \pm std, where geographically distinct areas are treated as the unit of replication. Dashed shape outlines indicate variables with records from <7 distinct geographic areas, and dashed arrows indicate fluxes with no data. To illustrate the magnitude of different fluxes, arrow size is proportional to the square root of corresponding flux. Asterisk after variable name indicates lack of C cycle closure.

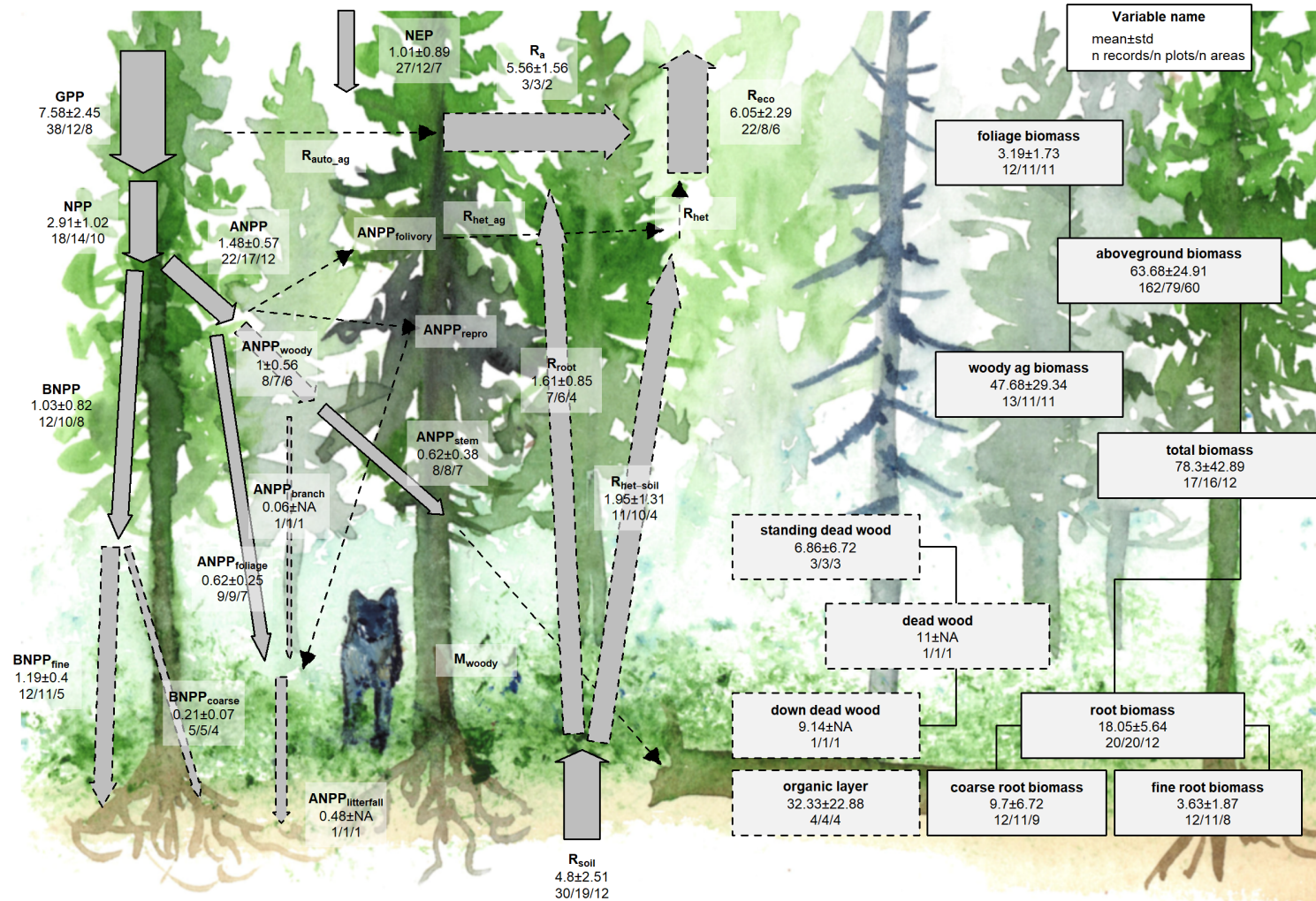


Figure 5 | C cycle diagram for mature boreal conifer forests. Arrows indicate fluxes ($\text{Mg C ha}^{-1} \text{ yr}^{-1}$); boxes indicate stocks (Mg C ha^{-1}), with variables as defined in Table 1. Presented are mean \pm std, where geographically distinct areas are treated as the unit of replication. Dashed shape outlines indicate variables with records from <7 distinct geographic areas, and dashed arrows indicate fluxes with no data. To illustrate the magnitude of different fluxes, arrow size is proportional to the square root of corresponding flux. Asterisk after variable name indicates lack of C cycle closure.

230 There were sufficient data to assess mature forest biome differences for 15 flux variables, and significant
231 differences among biomes were detected for 12 variables (Table 1). In all of these cases—including C fluxes
232 into, within, and out of the ecosystem—C fluxes were highest in tropical forests, intermediate in temperate
233 (broadleaf or conifer) forests, and lowest in boreal forests (Table 1, Figs. 6, S1-S15). Differences between
234 tropical and boreal forests were always significant, with temperate forests intermediate and significantly
235 different from one or both. Fluxes tended to be numerically greater in temperate broadleaf than conifer
236 forests, but the difference was never statistically significant. This pattern held for the following variables:
237 GPP , NPP , $ANPP$, $ANPP_{stem}$, $ANPP_{branch}$, $ANPP_{foliage}$, $BNPP$, R_{eco} , R_{root} , R_{soil} , and $R_{het-soil}$.
238 For two of the variables without significant differences among biomes ($ANPP_{litterfall}$ and $BNPP_{fine}$; Figs.
239 S8 and S11, respectively), the same general trends applied but were not statistically significant. Another
240 exception was for $BNPP_{root-coarse}$, where all records came from high-biomass forests in the US Pacific
241 Northwest, resulting in marginally higher values for the temperate conifer biome (Table 1, Fig. S10;
242 differences significant in mixed effects model but not in post-hoc pairwise comparison).

243 The most notable exception to the pattern of decreasing flux from tropical to boreal biomes was NEP , with
244 no significant differences across biomes but with the largest average in temperate broadleaf forests, followed
245 by tropical, boreal, and temperate conifer forests (Figs. 5,S1).

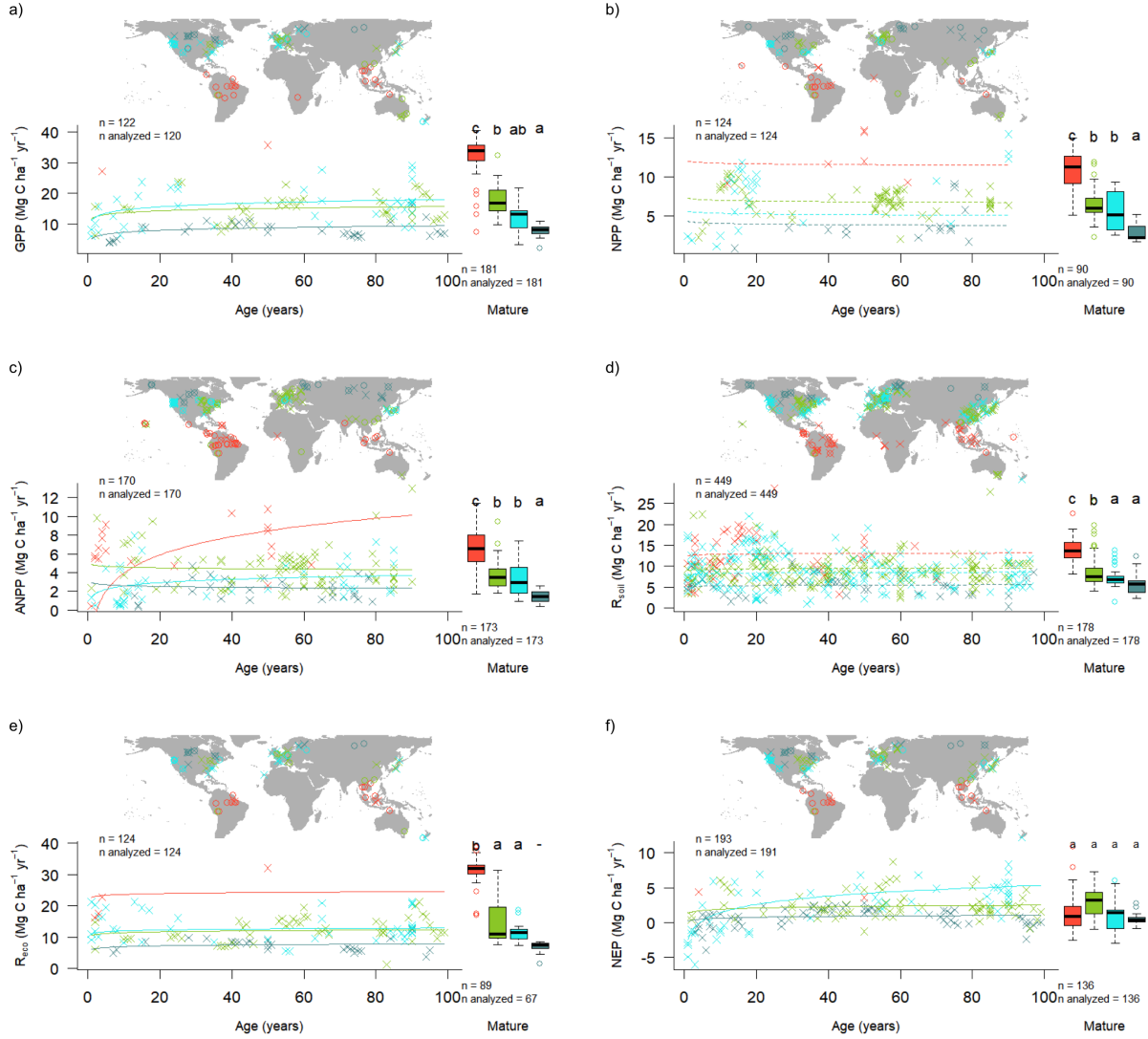


Figure 6 | Age trends and biome differences in some of the major C fluxes: (a) GPP , (b) NPP , (c) $ANPP$, (d) R_{soil} , (e) R_{eco} , and (f) NEP . Map shows data sources (x and o indicate young and mature stands, respectively). In each panel, the left scatterplot shows age trends in forests up to 100 years old, as characterized by a linear mixed effects model with fixed effects of age and biome. The fitted line indicates the effect of age on flux (solid lines: significant at $p < 0.05$, dashed lines: non-significant), and non-parallel lines indicate a significant age \times biome interaction. The boxplot illustrates distribution across mature forests, with different letters indicating significant differences between biomes. Data from biomes that did not meet the sample size criteria (see Methods) are plotted, but lack regression lines (young forests) or test of differences across biomes (mature forests). Individual figures for each flux with sufficient data are given in the Supplement (Figs. S1-S15).

246 There were sufficient data to assess mature forest biome differences for nine stock variables, and significant
 247 differences among biomes were detected for five variables (B_{tot} , B_{ag} , $B_{\text{ag-wood}}$, B_{foliage} , $B_{\text{root-coarse}}$; Table
 248 1). C stocks had less consistent patterns across biomes (Figs. 7, S16-S26). For B_{tot} and B_{ag} , tropical
 249 broadleaf forests had the highest biomass and boreal forests the lowest, with temperate broadleaf and
 250 needleleaf (B_{ag} only) intermediate. For three variables that had been disproportionately sampled in the
 251 high-biomass forests of the US Pacific Northwest ($B_{\text{ag-wood}}$, B_{foliage} , and $B_{\text{root-coarse}}$), temperate conifer
 252 forests had significantly higher stocks than the other biomes, which were not significantly different from one
 253 another.

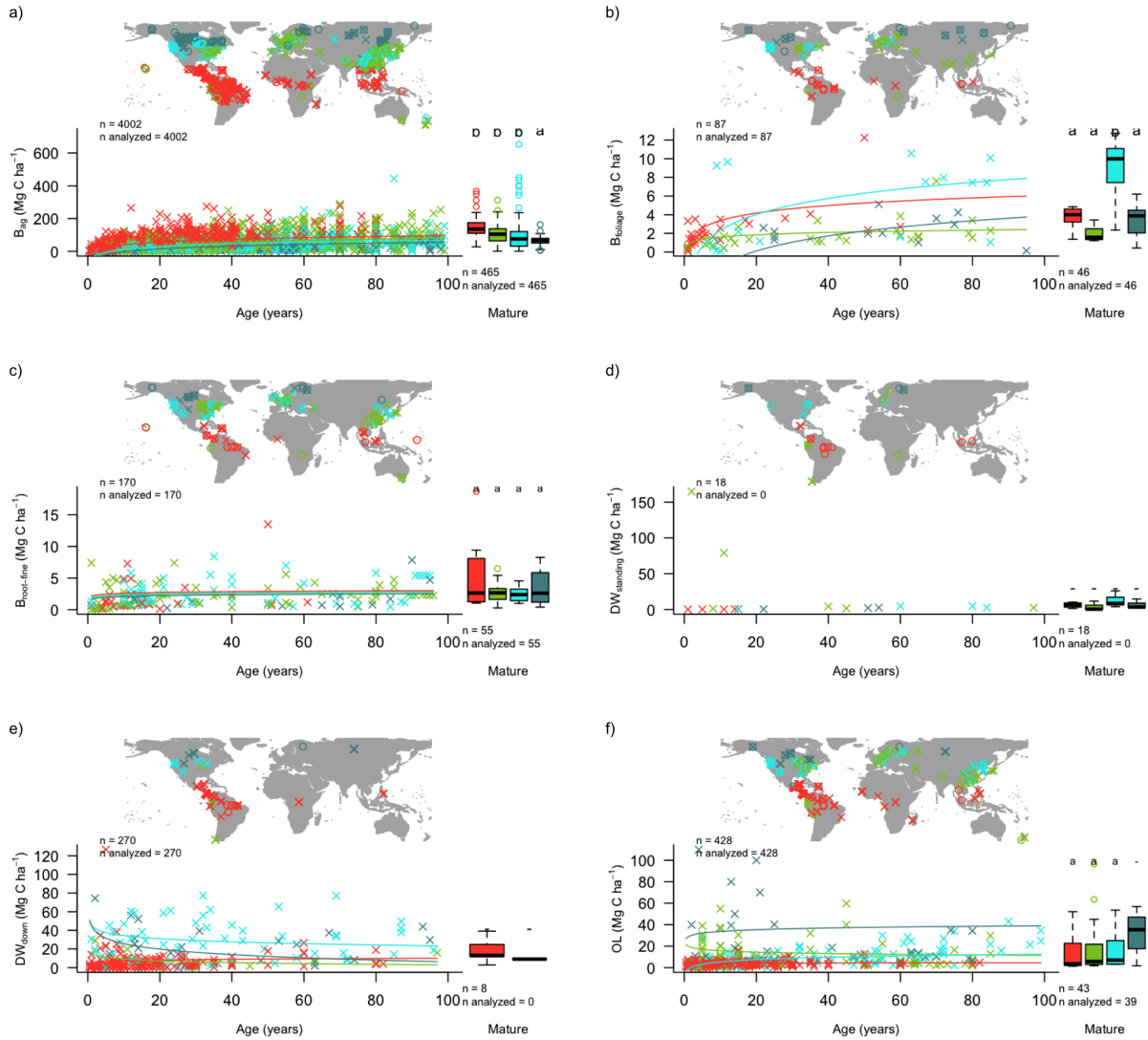


Figure 7 | Age trends and biome differences in some of the major forest C stocks: (a) aboveground biomass, (b) foliage, (c) fine roots, (d) dead wood. Map shows data sources (x and o indicate young and mature stands, respectively). In each panel, the left scatterplot shows age trends in forests up to 100 years old, as characterized by a linear mixed effects model with fixed effects of age and biome. The fitted line indicates the effect of age on flux (solid lines: significant at $p < 0.05$, dashed lines: non-significant), and non-parallel lines indicate a significant age \times biome interaction. The boxplot illustrates distribution across mature forests, with different letters indicating significant differences between biomes. Data from biomes that did not meet the sample size criteria (see Methods) are plotted, but lack regression lines (young forests) or test of differences across biomes (mature forests). Individual figures for each stock with sufficient data are given in the Supplement (Figs. S16-S26).

254 C cycling in young forests

255 Average C cycles for forests <100 years old are presented in Figures 8-11. Both C stocks and fluxes
 256 commonly increased significantly with stand age (Tables 1, S2, Figs. 6-11, S1-S26; detailed below).
 257 *ForC* contained 16 C flux variables with sufficient data for analyses of age trends in young forests (see
 258 Methods) (Figs. 6, S1-S15). Of these, ten increased significantly with age: *NEP*, *GPP*, *ANPP*,
 259 *ANPP_{woody}*, *ANPP_{foliage}*, *ANPP_{litterfall}*, *BNPP*, *BNPP_{fine}*, *R_{eco}*, and *R_{root}*. The remaining six—*NPP*,
 260 *ANPP_{stem}*, *ANPP_{branch}*, *BNPP_{coarse}*, *R_{soil-het}*, and *R_{soil-het}*—displayed no significant relationship to

261 stand age.

262 Differences in C fluxes across biomes typically paralleled those observed for mature forests, with C cycling
263 generally most rapid in the tropics and slowest in boreal forests. The single exception was $ANPP_{stem}$, for
264 which temperate broadleaf and conifer forests had similar flux rates than tropical forests. Notably, and in
265 contrast to the lack of biome differences in NEP for mature forests (Fig. 6), the tendency for temperate
266 forests to have greater fluxes than boreal forests held for NEP in regrowth forests (tropical forests excluded
267 because of insufficient data).

268 In terms of C stocks, ten variables (all but standing deadwood, $DW_{standing}$) had sufficient data to test for
269 age trends (Table 1, Figs. 7, S16-26). All of these displayed a significant overall increase with
270 $\log_{10}[stand.age]$. There were sufficient data to model age \times biome interactions were also significant for all
271 ten of these C stock variables (Table S2), with living C stocks tending to accumulate more rapidly during the
272 early stages of forest regrowth in tropical forests (Figs. 7, S16-S22). In the case of two non-living C stocks
273 (DW_{down} and OL), age \times biome interactions were such that Specifically, DW_{down} declined with age in
274 temperate and boreal forests, compared to an increase with age in tropical forests (Figs. 7, S25). Similarly,
275 OL declined slightly with age in temperate broadleaf forests, contrasting an increase in the other three
276 biomes (Figs. 7, S26).

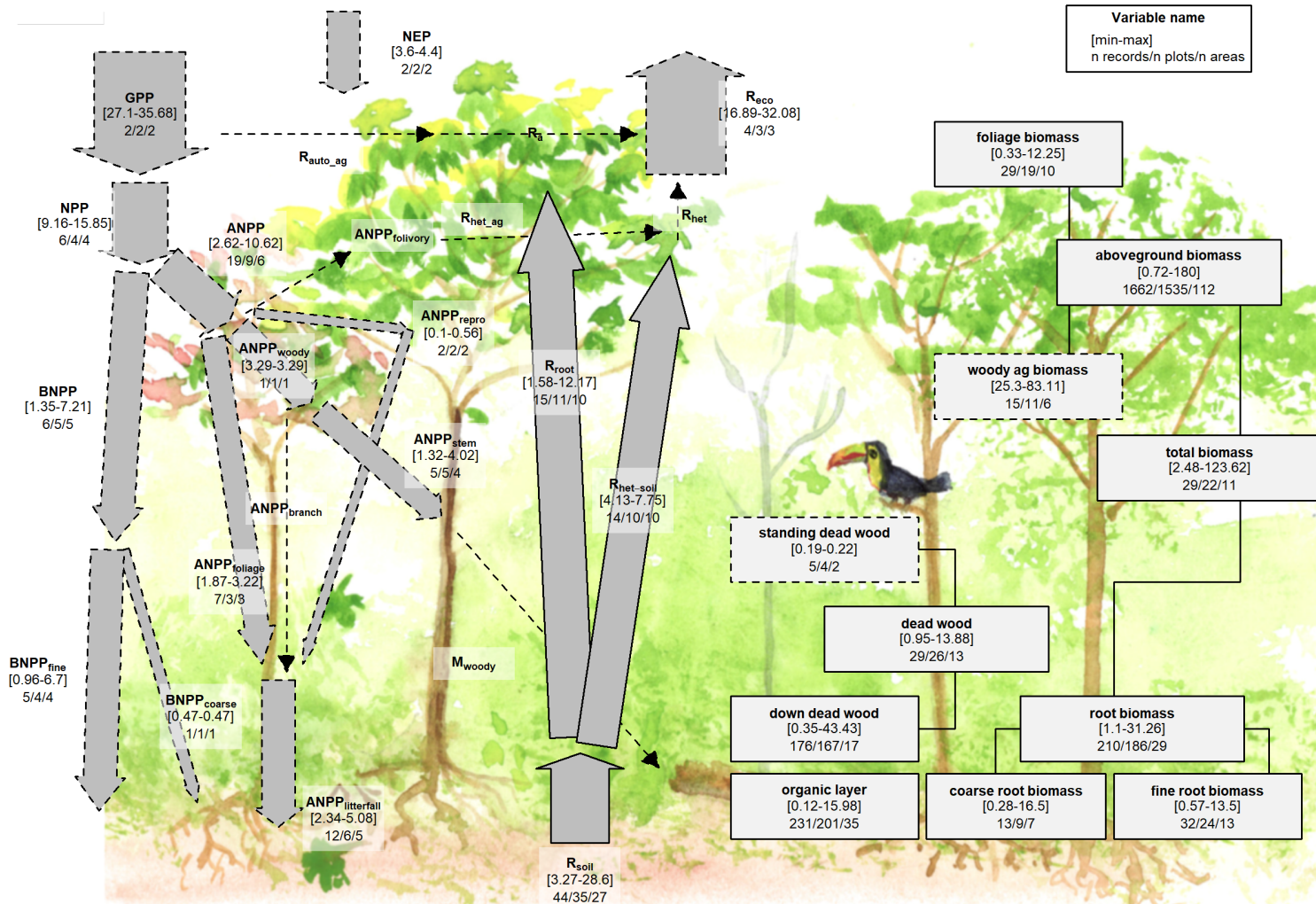


Figure 8 | C cycle diagram for young tropical broadleaf forests. Arrows indicate fluxes ($\text{Mg C ha}^{-1} \text{ yr}^{-1}$); boxes indicate stocks (Mg C ha^{-1}), with variables as defined in Table 1. Presented are observed ranges, where geographically distinct areas are treated as the unit of replication. All units are $\text{Mg C ha}^{-1} \text{ yr}^{-1}$ (fluxes) or Mg C ha^{-1} (stocks). Dashed shape outlines indicate variables with records from <7 distinct geographic areas, and dashed arrows indicate fluxes with no data. To illustrate the magnitude of different fluxes, arrow size is proportional to the square root of corresponding flux.

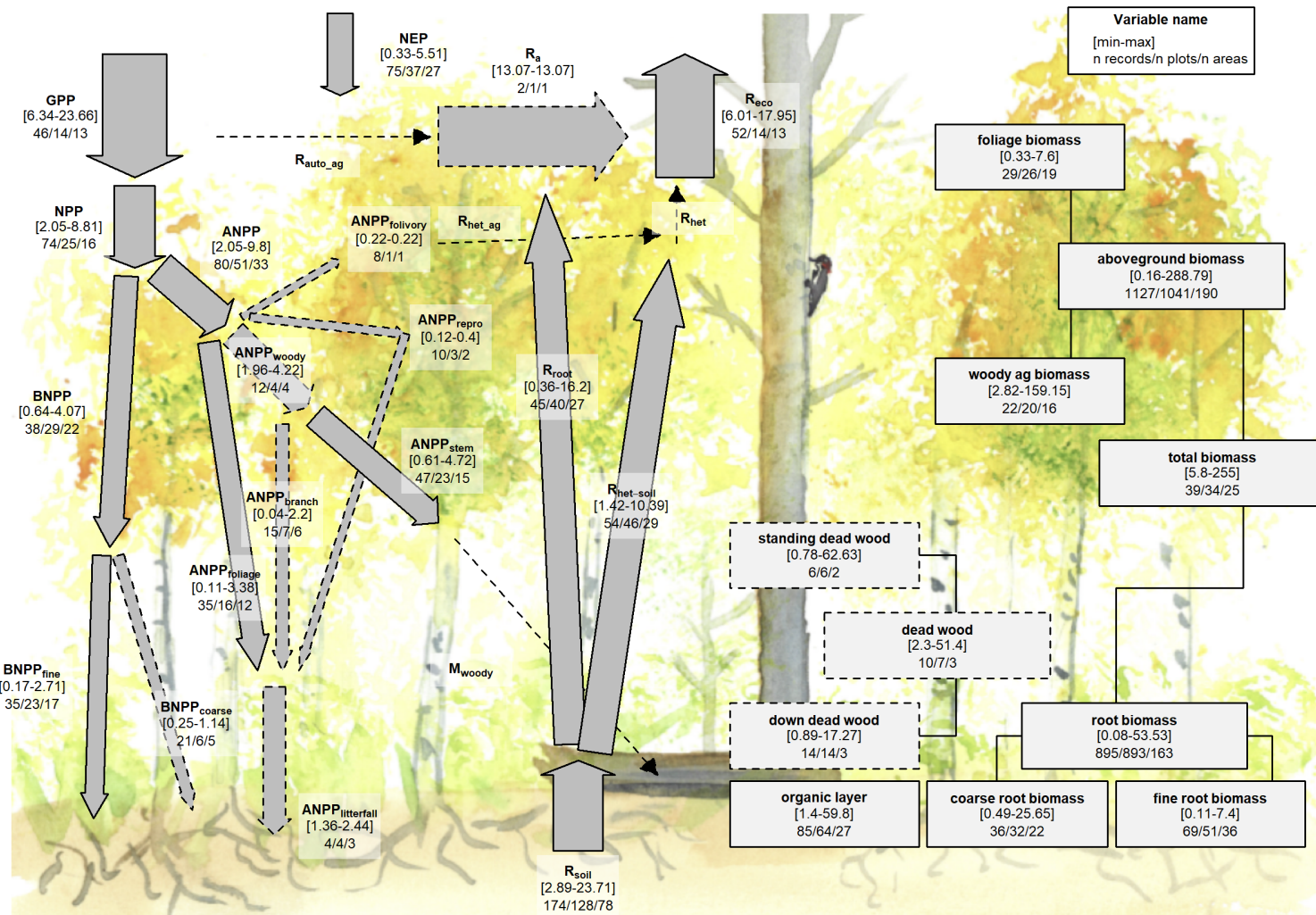


Figure 9 | C cycle diagram for young temperate broadleaf forests. Arrows indicate fluxes ($\text{Mg C ha}^{-1} \text{ yr}^{-1}$); boxes indicate stocks (Mg C ha^{-1}), with variables as defined in Table 1. Presented are observed ranges, where geographically distinct areas are treated as the unit of replication. All units are $\text{Mg C ha}^{-1} \text{ yr}^{-1}$ (fluxes) or Mg C ha^{-1} (stocks). Dashed shape outlines indicate variables with records from <7 distinct geographic areas, and dashed arrows indicate fluxes with no data. To illustrate the magnitude of different fluxes, arrow size is proportional to the square root of corresponding flux.

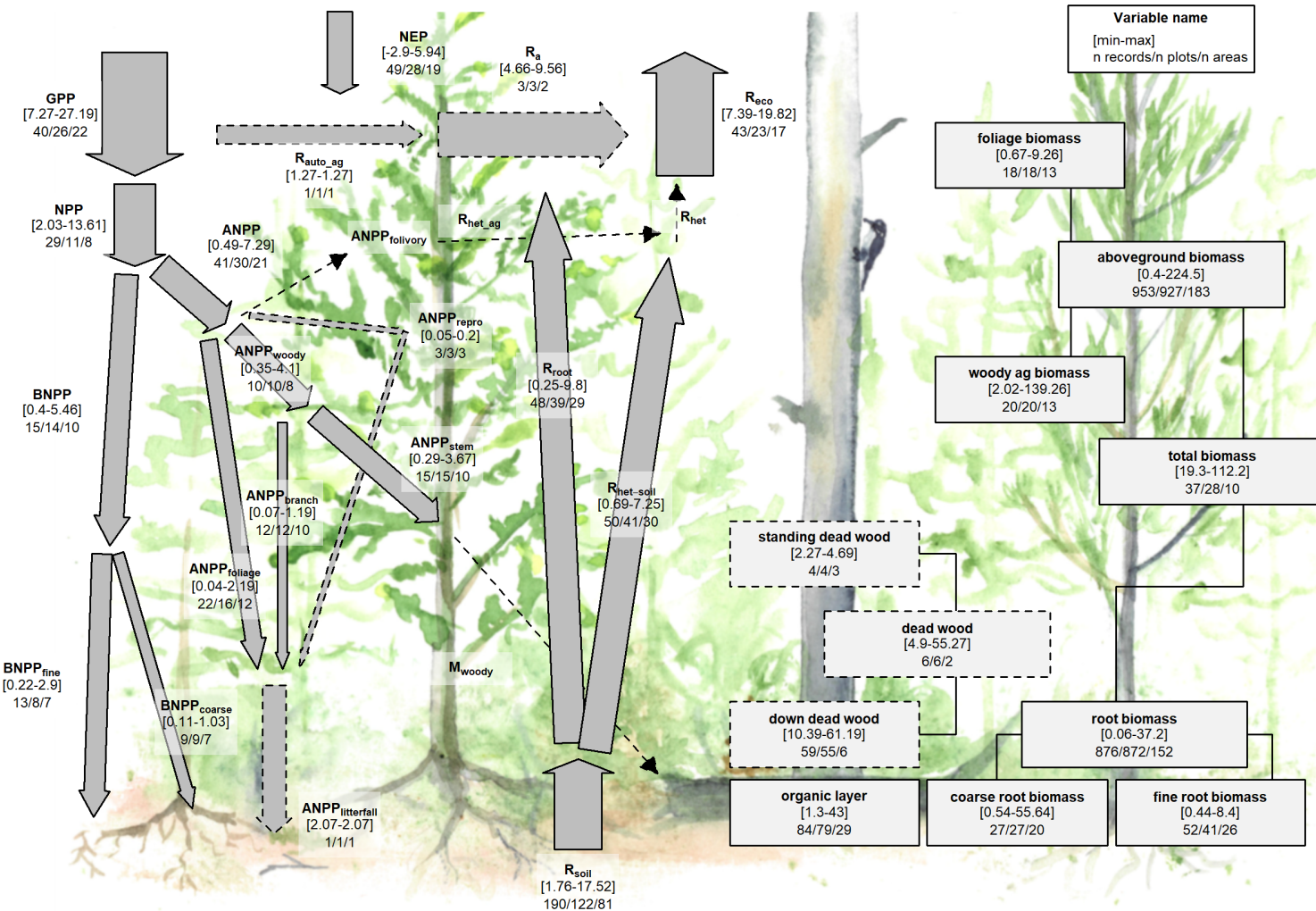


Figure 10 | C cycle diagram for young temperate conifer forests. Arrows indicate fluxes ($\text{Mg C ha}^{-1} \text{ yr}^{-1}$); boxes indicate stocks (Mg C ha^{-1}), with variables as defined in Table 1. Presented are observed ranges, where geographically distinct areas are treated as the unit of replication. All units are $\text{Mg C ha}^{-1} \text{ yr}^{-1}$ (fluxes) or Mg C ha^{-1} (stocks). Dashed shape outlines indicate variables with records from <7 distinct geographic areas, and dashed arrows indicate fluxes with no data. To illustrate the magnitude of different fluxes, arrow size is proportional to the square root of corresponding flux.

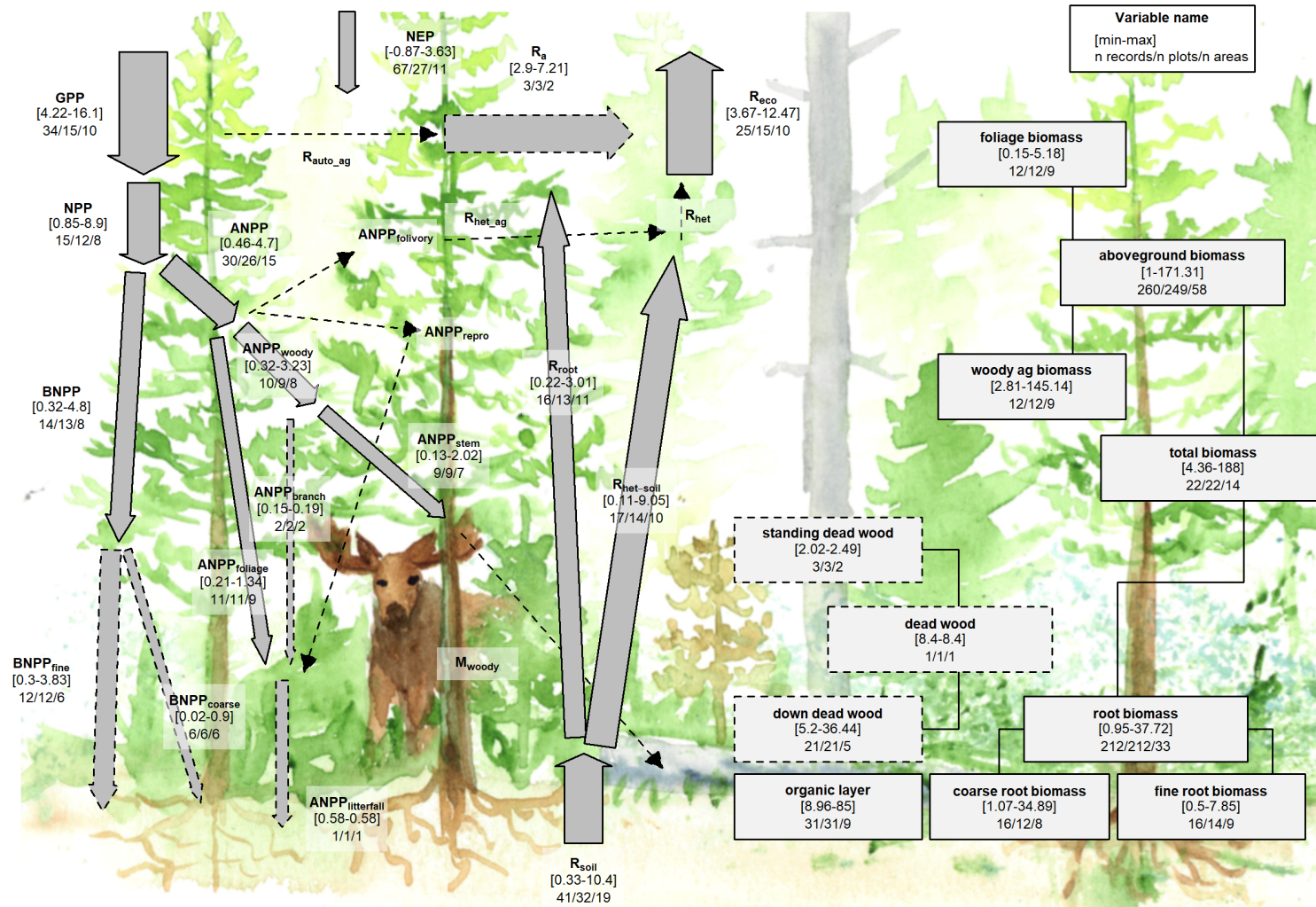


Figure 11 | C cycle diagram for young boreal conifer forests. Arrows indicate fluxes ($Mg\ C\ ha^{-1}\ yr^{-1}$); boxes indicate stocks ($Mg\ C\ ha^{-1}$), with variables as defined in Table 1. Presented are observed ranges, where geographically distinct areas are treated as the unit of replication. All units are $Mg\ C\ ha^{-1}\ yr^{-1}$ (fluxes) or $Mg\ C\ ha^{-1}$ (stocks). Dashed shape outlines indicate variables with records from <7 distinct geographic areas, and dashed arrows indicate fluxes with no data. To illustrate the magnitude of different fluxes, arrow size is proportional to the square root of corresponding flux.

277 **Discussion**

278 *ForC* v3.0 provided unprecedented coverage of most major variables, yielding an internally consistent picture
279 of C cycling in the world's major forest biomes. Carbon cycling rates generally increased from boreal to
280 tropical regions and with stand age. Specifically, the major C fluxes were highest in tropical forests,
281 intermediate in temperate (broadleaf or conifer) forests, and lowest in boreal forests – a pattern that generally
282 held for regrowth as well as mature forests (Figs. 6-7). In contrast to C fluxes, there was little directional
283 variation in mature forest C stocks across biomes (Figs. 2-5, 7). The majority of flux variables, together with
284 most live biomass pools, increased significantly with stand age (Figs. 6-11). Together, these results indicate
285 that, moving from cold to tropical climates and from young to old stands, there is a general acceleration of C
286 cycling, whereas C stocks and *NEP* of mature forests are correlated with a different set of factors.

287 **C variable coverage and budget closure**

288 The large number of C cycle variables covered by *ForC*, and the general consistency between them, provide
289 confidence that our overall reported means provide accurate and useful baselines for analysis – with the
290 caveats that they are unlikely to be accurate representations of C cycling for any particular forest, and that
291 these sample means almost certainly do not represent true biome means (particularly for temperate conifer
292 forests where high-biomass stands are over-represented in *ForC*).

293 There are of course notable holes in the *ForC* variable coverage (Fig. 1) that limit the scope of our inferences
294 here. Notably, *ForC* currently has sparse—if any—coverage of fluxes to herbivores and higher consumers, along
295 with the woody mortality (M_{woody}) and dead wood stocks (Tables 1, Figs. S23-S25). Geographically, all
296 variables are poorly covered in Africa and Siberia, a common problem in the carbon-cycle community (Xu
297 and Shang 2016, Schimel *et al* 2015). *ForC* does not include soil carbon, which is covered by other efforts
298 (e.g., Köchy *et al* 2015). *ForC* is not intended to replace databases that are specialized for particular parts of
299 the C cycle analyses, e.g., aboveground biomass (Spawn *et al* 2020), land-atmosphere fluxes (Baldocchi *et al*
300 2001), soil respiration (Jian *et al* 2020), or the human footprint in global forests (Magnani *et al* 2007).

301 In this analysis, the C cycle budgets for mature forests (Figs. 2-5) generally “close”—that is, the sums of
302 component variables do not differ from the larger fluxes by more than one standard deviation. On the one
303 hand, this reflects the general fact that ecosystem-scale measurements tend to close the C budget more easily
304 and consistently than, for example, for energy balance (Stoy *et al* 2013). On the other, however, *ForC*
305 derives data from multiple heterogeneous sources, and standard deviations within each biome are high; as a
306 result, the standard for C closure is relatively loose (*c.f.* Houghton 2020). Nonetheless, the lack of closure, in
307 the one instance where it occurs, is probably more reflective of differences in the representation of forest
308 types (*i.e.*, disproportionate representation of US Pacific NW for $B_{root-coarse}$ relative to B_{root} ; Fig. 4) than
309 of methodological accuracy. The overall high degree of closure implies that *ForC* gives a consistent picture of
310 C cycling within biomes. This is an important and useful test, because it allows for consistency checks within
311 the C cycle, for example leveraging separate and independently-measured fluxes to constrain errors in
312 another (Phillips *et al* 2017, Williams *et al* 2014, Harmon *et al* 2011), or producing internally consistent
313 global data products (Wang *et al* 2018).

314 **C cycling across biomes**

315 Our analysis reveals that carbon cycling is most rapid in the tropics and slowest in boreal regions, including
316 C fluxes into (GPP), within (e.g., NPP and its components), and out of (e.g., R_{soil} , R_{eco}) the ecosystem.

317 For mature forests, this is consistent with a large body of previous work demonstrating that C fluxes
318 generally decline with latitude (or increase with temperature) on a global scale (e.g., Luyssaert *et al* 2007,
319 Gillman *et al* 2015, Li and Xiao 2019, Banbury Morgan *et al* n.d.). The consistency with which this occurs
320 across numerous fluxes is not surprising, but has never been simultaneously assessed across such a large
321 number of variables (but see Banbury Morgan *et al* n.d. for nine autotrophic fluxes).

322 The notable exception to the pattern of fluxes decreasing from tropical to boreal regions is NEP (Fig. 6f),
323 which showed no significant differences across biomes. Unlike the other C flux variables, NEP does not
324 characterize the rate at which C cycles through the ecosystem, but is the balance between C sequestration
325 (GPP) and respiratory losses (R_{eco}) and represents net CO₂ sequestration (or release) by the ecosystem.
326 NEP tends to be relatively small in mature forest stands (discussed further below), which accumulate
327 carbon slowly relative to younger stands, if at all (Luyssaert *et al* 2008, Amiro *et al* 2010, Besnard *et al*
328 2018). It is therefore unsurprising that there are no pronounced differences across biomes, suggesting that
329 variation in NEP of mature forests is controlled less by climate and more by other factors including
330 moderate disturbances (Curtis and Gough 2018) or disequilibrium of R_{soil} relative to C inputs (e.g., in
331 peatlands where anoxic conditions inhibit decomposition; Wilson *et al* 2016).

332 In contrast to the patterns observed for NEP in mature stands, NEP of stands between 20 and 100 years of
333 age varied across biomes, being lowest in boreal forests, intermediate in temperate broadleaf forests, and
334 highest in temperate conifer forests (with insufficient data to assess tropical forests; Figs. 6f, S1). This is
335 consistent with findings that live biomass accumulation rates (e.g., ΔB_{ag} or ΔB_{tot}) during early secondary
336 succession decrease with latitude (Figs. 7a, S16-S22; Anderson *et al* 2006, Cook-Patton *et al* 2020). Note,
337 though, that NEP includes not only ΔB_{tot} , but also changes in DW_{tot} , OL , and soil carbon, and biome
338 differences in the accumulation rates of these variables have not been detected, in part because these
339 variables do not consistently increase with stand age (Figs. 7, S23-S26, and see discussion below;
340 Cook-Patton *et al* 2020).

341 For regrowth forests, little is known about cross-biome differences in carbon fluxes, and we are not aware of
342 any previous large-scale comparisons of C fluxes that have been limited to regrowth forests. Thus, this
343 analysis was the first to examine flux trends in regrowth forests across biomes. The observed tendency for
344 young forest fluxes to decrease from tropical to boreal regions paralleled patterns in mature forests (Figs. 6,
345 S1-S15), suggesting that regrowth forests follow latitudinal trends in carbon cycling similar to those of
346 mature forests (e.g., Banbury Morgan *et al* n.d.).

347 In contrast to C fluxes and biomass accumulation rates in regrowth forests, stocks showed less systematic
348 variation across biomes. For aboveground biomass, which is the variable in *ForC* with broadest geographical
349 representation, the modest trend of declining biomass from tropical to boreal regions mirrors observations
350 from spaceborne lidar that reveal a decline in aboveground biomass (for all forests, including secondary) with
351 latitude across the N hemisphere (Hu *et al* 2016). The highest- biomass forests on Earth are, however, found
352 in coastal temperate climates of both the southern and northern hemisphere (Keith *et al* 2009, Smithwick *et*
353 *al* 2002, Hu *et al* 2016). Disproportionate representation of forests in one such region—the US Pacific
354 Northwest—inflated estimates of temperate conifer fluxes and stocks for some variables and was responsible

355 for all of the anomalous results described here (e.g., lack of complete C budget closure, anomalous trend
356 across biomes for $BNPP_{coarse}$). Thus, biome differences should always be interpreted relative to the
357 geographic distribution of sampling, which only rarely covers the majority of forested area within a biome.
358 Whereas biomass can be remotely sensed and receives significant research attention, far less is known about
359 geographical variation in deadwood and organic layer (OL) across biomes, which has proved a limitation for
360 C accounting efforts (Pan *et al* 2011). Although these stocks can be important—exceeding 100 Mg C ha⁻¹ in
361 some stands (Figs. 7d-e, S23-S25), this study is the first to synthesize deadwood data on a global scale (but
362 see Cook-Patton *et al* 2020 for young forests). Unfortunately, data remain too sparse for statistical
363 comparison across biomes (Figs. 7, S23-S25; but see below for age trends), pointing to a need for more
364 widespread quantification of both standing and downed deadwood. *ForC* coverage of OL stocks is more
365 comprehensive, revealing no significant differences across temperate and tropical biomes, but a tendency
366 towards higher OL in boreal forests, consistent with the idea that slower decomposition in colder climates
367 results in more buildup of organic matter (Allen *et al* 2002). Further research on non-living C stocks in the
368 world's forests will be essential to completing the picture.

369 Age trends in C cycling

370 Our study reveals that most C fluxes quickly increase to a plateau as stands age (Fig. 6), consistent with
371 current understanding of age trends in forest C cycling (e.g., Anderson-Teixeira *et al* 2013, Amiro *et al* 2010,
372 Magnani *et al* 2007). While limited records in very young (*i.e.*, <5 year old) stands resulted in poor
373 resolution of the earliest phases of this increase for many variables (sometimes detecting no age trend; Table
374 1), any autotrophic C flux (e.g., GPP , NPP and its components, R_{auto}) would be minimal immediately
375 following a stand-clearing disturbance. These would be expected to increase rapidly with the most
376 metabolically active components of biomass, foliage and fine roots, which also increase rapidly with stand age
377 (Fig. 7). In contrast, soil heterotrophic respiration ($R_{het-soil}$) and total soil respiration (R_{soil}) are expected
378 to be non-zero following stand-clearing disturbance, although these may decrease with a reduction of root
379 respiration (R_{soil} only) and C exudates or increase in response to an influx of dead roots and litter
380 (Ribeiro-Kumara *et al* 2020, Maurer *et al* 2016, Bond-Lamberty *et al* 2004). In this study, we detect no
381 significant age trends in either variable.

382 Notably, net carbon sequestration (NEP) increases with age up to the 100-yr threshold examined here, with
383 more pronounced patterns in temperate than boreal forests (Fig. 6f). This finding is largely consistent with,
384 but built from a far larger dataset than, previous studies showing an increase in NEP across relatively
385 young stand ages (Pregitzer and Euskirchen 2004, Baldocchi *et al* 2001, Luyssaert *et al* 2008). However,
386 NEP has been observed to decline from intermediate to old stands (Luyssaert *et al* 2008), and the NEP
387 estimated by our model for 100-year-old temperate conifer stands (~5 Mg C ha⁻¹ yr⁻¹) exceeds the mean of
388 mature forests in the same biome (0.7 Mg C ha⁻¹ yr⁻¹; Fig. 4). A decrease in NEP is consistent with the
389 observed deceleration of biomass accumulation as stands age, although both biomass and non-living C stocks
390 will often continue to increase well beyond the 100-yr threshold used here to delimit young and mature
391 stands (Luyssaert *et al* 2008, McGarvey *et al* 2014, Lichstein *et al* 2009).

392 In terms of stocks, our study reveals consistent increases in live biomass stocks with stand age—a pattern that
393 is well-known and expected (e.g., Lichstein *et al* 2009, Yang *et al* 2011)—and more variable age trends in
394 deadwood and OL . The latter are particularly sensitive to the type of disturbance, where disturbances that
395 remove most organic material (e.g., logging, agriculture) result in negligible deadwood in young stands,

followed by a buildup over time (tropical stands in Fig. 7e; e.g., Vargas *et al* 2008). In contrast, natural disturbances (e.g., fire, drought) can produce large amounts of deadwood (mostly $DW_{standing}$) that slowly decomposes as the stand recovers, resulting in declines across young stand ages (e.g., temperate and boreal stands in Fig. 7e; e.g., Carmona *et al* 2002). Again, further study and synthesis of non-living C stocks across biomes and stand ages will be valuable to giving a more comprehensive picture.

Relevance for climate change prediction and mitigation

The future of forest C cycling (Song *et al* 2019) will shape trends in atmospheric CO₂ and the course of climate change (Schimel *et al* 2015). Our findings, and more generally the data contained in *ForC* and summarized here, can help to meet two major challenges.

First, improved representation of forest C cycling in models is essential to improving predictions of the future course of climate change, for the simple reason that by definition future projections extend our existing observations and understanding to conditions that do not currently exist on Earth (McDowell *et al* 2018, Bonan and Doney 2018, Gustafson *et al* 2018). To ensure that models are giving the right answers for the right reasons (Sulman *et al* 2018), it is important to benchmark against multiple components of the C cycle that are internally consistent with each other (Collier *et al* 2018, Wang *et al* 2018). *ForC*'s tens of thousands of records are readily available in a standardized format, and our analyses here indicate that their internal consistency is reasonably high. Integration of *ForC* with models will be valuable to improving the accuracy and reliability of models.

Second, *ForC* can serve as a pipeline through which information can flow efficiently from forest researchers to decision-makers working to implement forest conservation strategies at global, national, or landscape scales. This is already happening: *ForC* has contributed to updating the IPCC guidelines for carbon accounting in forests (IPCC 2019, Requena Suarez *et al* 2019), mapping C accumulation potential from natural forest regrowth globally (Cook-Patton *et al* 2020), and informing ecosystem conservation priorities (Goldstein *et al* 2020).

It is also interesting to consider the complementary utility of global-scale but spatially discontinuous databases such as *ForC* and remote wall-to-wall remote sensing products. The latter provide unparalleled insight into aboveground carbon stocks, but less constraint on belowground stocks or carbon fluxes in general (Bond-Lamberty *et al* 2016, Anav *et al* 2015). Combining observational data and remote observations may provide a much more comprehensive and accurate picture of global forest C cycling, particularly when used in formal data assimilation systems (Konings *et al* 2019, Liu *et al* 2018). Biomass is the largest C stock in most forests, and most of the emphasis has traditionally been on this variable. Remote-sensing driven biomass estimates (e.g., Saatchi *et al* 2011), calibrated based on high-quality ground-based data (Schepaschenko *et al* 2019, Chave *et al* 2019), are well suited for this task. Note, however, that factors such as stand age and disturbance history are difficult, if possible, to detect remotely, and can only be characterized for very recent decades (Hansen *et al* 2013, Song *et al* 2018, Curtis *et al* 2018). Ground-based data such as *ForC* are therefore valuable in defining age-based trajectories in biomass, as in Cook-Patton *et al* (2020), and thus constraining variables such as carbon sink potential (Luyssaert *et al* 2008).

In contrast, carbon allocation within forest ecosystems and respiration fluxes cannot be remotely sensed. Efforts such as the Global Carbon Project (Friedlingstein *et al* 2019) and NASA's Carbon Monitoring System (Liu *et al* 2018) typically compute respiration as residuals of all other terms (Bond-Lamberty *et al*

436 2016, Harmon *et al* 2011). This means that the errors on respiration outputs are likely to be large and
437 certainly poorly constrained, offering a unique opportunity for databases such as ForC and SRDB (Jian *et al*
438 2020) to provide observational benchmarks. For example, Konings *et al* (2019) produced a unique top-down
439 estimate of global heterotrophic respiration that can both be compared with extant bottom-up estimates
440 (Bond-Lamberty 2018) and used as an internal consistency check on other parts of the carbon cycle (Phillips
441 *et al* 2017).

442 **Conclusions**

443 As climate change accelerates, understanding and managing the carbon dynamics of forests—notably
444 including dynamics and fluxes that cannot be observed by satellites—is critical to forecasting, mitigation, and
445 adaptation. The C data in *ForC*, as summarized here, will be valuable to these efforts. Notably, the fact that
446 tropical forests tend to have both the highest rates of C sequestration in young stands (Fig. 7; Cook-Patton
447 *et al* 2020), fueled by their generally high C flux rates (Table 1; Fig. 6), and the highest mean biomass (Fig.
448 7; Table 1; Hu *et al* 2016, Jian *et al* 2020) reinforces the concept that conservation and restoration of these
449 forests is a priority for climate change mitigation, along with high-biomass old-growth temperate stands
450 (Grassi *et al* 2017, Goldstein *et al* 2020). It is also important to note the trade-off in climate mitigation
451 potential of restoration of young forests, with high rates of CO₂ sequestration (*NEP*; Cook-Patton *et al*
452 2020), versus conservation and management of mature forests, with low *NEP* but high C stocks that could
453 not be recovered on a time scale relevant to climate change mitigation (Goldstein *et al* 2020). Generally
454 speaking, the conservation of mature forests will yield greater climate benefits (Anderson-Teixeira and
455 DeLucia 2011), but both approaches are critical to avoiding catastrophic climate change (IPCC 2018).

456 **Acknowledgements**

457 Thanks to all researchers whose data are included in *ForC* and this analysis, to Jennifer McGarvey and Ian
458 McGregor for help with the database, and to Norbert Kunert for helpful discussion. Funding sources
459 included a Smithsonian Scholarly Studies grant to KAT and HML and a Smithsonian Working Land and
460 Seascapes grant to KAT.

461 **Data availability statement**

462 Materials required to fully reproduce these analyses, including data, R scripts, and image files, are archived
463 in Zenodo [DOI: TBD]. Data, scripts, and results presented here are also available through the open-access
464 *ForC* GitHub repository (<https://github.com/forc-db/ForC>), where many will be updated as the database
465 develops.

466 **References**

- 467 Allen A, Brown J and Gillooly J 2002 Global biodiversity, biochemical kinetics, and the energetic-equivalence
468 rule *SCIENCE* **297** 1545–8 Online: <http://linkseeker.lanl.gov/unm?genre=article&issn=0036-8075&date=2002&volume=297&issue=5586&spage=1545&atitle=Global+biodiversity%2C+biochemical+kinetics%2C+and+the+energetic%2Dequivalence+rule&aulast=Allen&auinit=AP>
- 471 Amiro B D, Barr A G, Barr J G, Black T A, Bracho R, Brown M, Chen J, Clark K L, Davis K J, Desai A R,
472 Dore S, Engel V, Fuentes J D, Goldstein A H, Goulden M L, Kolb T E, Lavigne M B, Law B E, Margolis H

- 473 A, Martin T, McCaughey J H, Misson L, Montes-Helu M, Noormets A, Randerson J T, Starr G and Xiao J
 474 2010 Ecosystem carbon dioxide fluxes after disturbance in forests of North America *Journal of Geophysical*
 475 *Research: Biogeosciences* **115** Online:
 476 <http://agupubs.onlinelibrary.wiley.com/doi/abs/10.1029/2010JG001390>
- 477 Anav A, Friedlingstein P, Beer C, Ciais P, Harper A, Jones C, Murray-Tortarolo G, Papale D, Parazoo N C,
 478 Peylin P, Piao S, Sitch S, Viovy N, Wiltshire A and Zhao M 2015 Spatiotemporal patterns of terrestrial gross
 479 primary production: A review *Reviews of Geophysics* **53** 785–818 Online:
 480 <http://agupubs.onlinelibrary.wiley.com/doi/abs/10.1002/2015RG000483>
- 481 Andela N, Morton D C, Giglio L, Chen Y, Werf G R van der, Kasibhatla P S, DeFries R S, Collatz G J,
 482 Hantson S, Kloster S, Bachelet D, Forrest M, Lasslop G, Li F, Mangeon S, Melton J R, Yue C and
 483 Randerson J T 2017 A human-driven decline in global burned area *Science* **356** 1356–62 Online:
 484 <http://science.sciencemag.org/content/356/6345/1356>
- 485 Anderson K J, Allen A P, Gillooly J F and Brown J H 2006 Temperature-dependence of biomass
 486 accumulation rates during secondary succession *Ecology Letters* **9** 673–82 Online:
 487 <http://www.blackwell-synergy.com/doi/abs/10.1111/j.1461-0248.2006.00914.x>
- 488 Anderson-Teixeira K, Herrmann V, CookPatton, Ferson A and Lister K 2020 Forc-db/GROA: Release with
 489 Cook-Patton et al. 2020, Nature. Online: <https://zenodo.org/record/3983644>
- 490 Anderson-Teixeira K J, Davies S J, Bennett A C, Gonzalez-Akre E B, Muller-Landau H C, Joseph Wright S,
 491 Abu Salim K, Almeyda Zambrano A M, Alonso A, Baltzer J L, Basset Y, Bourg N A, Broadbent E N,
 492 Brockelman W Y, Bunyavejchewin S, Burslem D F R P, Butt N, Cao M, Cardenas D, Chuyong G B, Clay K,
 493 Cordell S, Dattaraja H S, Deng X, Detto M, Du X, Duque A, Erikson D L, Ewango C E N, Fischer G A,
 494 Fletcher C, Foster R B, Giardina C P, Gilbert G S, Gunatilleke N, Gunatilleke S, Hao Z, Hargrove W W,
 495 Hart T B, Hau B C H, He F, Hoffman F M, Howe R W, Hubbell S P, Inman-Narahari F M, Jansen P A,
 496 Jiang M, Johnson D J, Kanzaki M, Kassim A R, Kenfack D, Kibet S, Kinnaird M F, Korte L, Kral K,
 497 Kumar J, Larson A J, Li Y, Li X, Liu S, Lum S K Y, Lutz J A, Ma K, Maddalena D M, Makana J-R, Malhi
 498 Y, Marthews T, Mat Serudin R, McMahon S M, McShea W J, Memiaghe H R, Mi X, Mizuno T, Morecroft
 499 M, Myers J A, Novotny V, Oliveira A A de, Ong P S, Orwig D A, Ostertag R, Ouden J den, Parker G G,
 500 Phillips R P, Sack L, Sainge M N, Sang W, Sri-ngernyuang K, Sukumar R, Sun I-F, Sungpalee W, Suresh H
 501 S, Tan S, Thomas S C, Thomas D W, Thompson J, Turner B L, Uriarte M, Valencia R, et al 2015
 502 CTFS-ForestGEO: A worldwide network monitoring forests in an era of global change *Global Change Biology*
 503 **21** 528–49 Online: <http://onlinelibrary.wiley.com/doi/10.1111/gcb.12712/abstract>
- 504 Anderson-Teixeira K J and DeLucia E H 2011 The greenhouse gas value of ecosystems *Global Change Biology*
 505 **17** 425–38 Online: <http://doi.wiley.com/10.1111/j.1365-2486.2010.02220.x>
- 506 Anderson-Teixeira K J, Miller A D, Mohan J E, Hudiburg T W, Duval B D and DeLucia E H 2013 Altered
 507 dynamics of forest recovery under a changing climate *Global Change Biology* **19** 2001–21 Online:
 508 <http://onlinelibrary.wiley.com/doi/abs/10.1111/gcb.12194>
- 509 Anderson-Teixeira K J, Wang M M H, McGarvey J C, Herrmann V, Tepley A J, Bond-Lamberty B and
 510 LeBauer D S 2018 ForC: A global database of forest carbon stocks and fluxes *Ecology* **99** 1507–7 Online:
 511 <http://doi.wiley.com/10.1002/ecy.2229>
- 512 Anderson-Teixeira K J, Wang M M H, McGarvey J C and LeBauer D S 2016 Carbon dynamics of mature

- 513 and regrowth tropical forests derived from a pantropical database (TropForC-db) *Global Change Biology* **22**
 514 1690–709 Online: <http://onlinelibrary.wiley.com/doi/10.1111/gcb.13226/abstract>
- 515 Badgley G, Anderegg L D L, Berry J A and Field C B 2019 Terrestrial gross primary production: Using
 516 NIRV to scale from site to globe *Global Change Biology* **25** 3731–40 Online:
 517 <http://onlinelibrary.wiley.com/doi/abs/10.1111/gcb.14729>
- 518 Baldocchi D, Falge E, Gu L, Olson R, Hollinger D, Running S, Anthoni P, Bernhofer C, Davis K, Evans R,
 519 Fuentes J, Goldstein A, Katul G, Law B, Lee X, Malhi Y, Meyers T, Munger W, Oechel W, Paw K T,
 520 Pilegaard K, Schmid H P, Valentini R, Verma S, Vesala T, Wilson K and Wofsy S 2001 FLUXNET: A New
 521 Tool to Study the Temporal and Spatial Variability of Ecosystem-Scale Carbon Dioxide, Water Vapor, and
 522 Energy Flux Densities *Bulletin of the American Meteorological Society* **82** 2415–34 Online:
 523 [http://journals.ametsoc.org/doi/abs/10.1175/1520-0477\(2001\)082%3C2415:FANTTS%3E2.3.CO;2](http://journals.ametsoc.org/doi/abs/10.1175/1520-0477(2001)082%3C2415:FANTTS%3E2.3.CO;2)
- 524 Banbury Morgan B, Herrmann V, Kunert N, Bond-Lamberty B, Muller-Landau H C and Anderson-Teixeira
 525 K J Global patterns of forest autotrophic carbon fluxes *Global Change Biology*
- 526 Bates D, Mächler M, Bolker B and Walker S 2015 Fitting Linear Mixed-Effects Models Using **lme4** *Journal*
 527 *of Statistical Software* **67** Online: <http://www.jstatsoft.org/v67/i01/>
- 528 Besnard S, Carvalhais N, Arain M A, Black A, Bruun S de, Buchmann N, Cescatti A, Chen J, Clevers J G P
 529 W, Desai A R, Gough C M, Havrankova K, Herold M, Hörtnagl L, Jung M, Knohl A, Kruijt B, Krupkova L,
 530 Law B E, Lindroth A, Noormets A, Roupsard O, Steinbrecher R, Varlagin A, Vincke C and Reichstein M
 531 2018 Quantifying the effect of forest age in annual net forest carbon balance *Environmental Research Letters*
 532 **13** 124018 Online: <https://iopscience.iop.org/article/10.1088/1748-9326/aaeaeb>
- 533 Bonan G B 2008 Forests and Climate Change: Forcings, Feedbacks, and the Climate Benefits of Forests
 534 *Science* **320** 1444–9 Online: <http://www.sciencemag.org/cgi/content/abstract/320/5882/1444>
- 535 Bonan G B and Doney S C 2018 Climate, ecosystems, and planetary futures: The challenge to predict life in
 536 Earth system models *Science* **359** Online: <http://science.sciencemag.org/content/359/6375/eaam8328>
- 537 Bonan G B, Lombardozzi D L, Wieder W R, Oleson K W, Lawrence D M, Hoffman F M and Collier N 2019
 538 Model Structure and Climate Data Uncertainty in Historical Simulations of the Terrestrial Carbon Cycle
 539 (1850–2014) *Global Biogeochemical Cycles* **33** 1310–26 Online:
 540 <https://onlinelibrary.wiley.com/doi/abs/10.1029/2019GB006175>
- 541 Bond-Lamberty B 2018 New Techniques and Data for Understanding the Global Soil Respiration Flux
 542 *Earth's Future* **6** 1176–80 Online: <http://agupubs.onlinelibrary.wiley.com/doi/abs/10.1029/2018EF000866>
- 543 Bond-Lamberty B, Epron D, Harden J, Harmon M E, Hoffman F, Kumar J, David McGuire A and Vargas R
 544 2016 Estimating heterotrophic respiration at large scales: Challenges, approaches, and next steps *Ecosphere*
 545 **7** Online: <https://onlinelibrary.wiley.com/doi/abs/10.1002/ecs2.1380>
- 546 Bond-Lamberty B and Thomson A 2010 A global database of soil respiration data *Biogeosciences* **7** 1915–26
 547 Online: <http://www.biogeosciences.net/7/1915/2010/>
- 548 Bond-Lamberty B, Wang C and Gower S T 2004 Contribution of root respiration to soil surface CO₂ flux in
 549 a boreal black spruce chronosequence *Tree Physiology* **24** 1387–95 Online:
 550 <http://academic.oup.com/treephys/article/24/12/1387/1612153>

- 551 Carmona M R, Armesto J J, Aravena J C and Pérez C A 2002 Coarse woody debris biomass in successional
 552 and primary temperate forests in Chiloé Island, Chile *Forest Ecology and Management* **164** 265–75 Online:
 553 <http://www.sciencedirect.com/science/article/pii/S0378112701006028>
- 554 Cavalieri M A, Reed S C, Smith W K and Wood T E 2015 Urgent need for warming experiments in tropical
 555 forests *Global Change Biology* **21** 2111–21 Online:
 556 <http://onlinelibrary.wiley.com/doi/10.1111/gcb.12860/abstract>
- 557 Chave J, Davies S J, Phillips O L, Lewis S L, Sist P, Schepaschenko D, Armston J, Baker T R, Coomes D,
 558 Disney M, Duncanson L, Hérault B, Labrière N, Meyer V, Réjou-Méchain M, Scipal K and Saatchi S 2019
 559 Ground Data are Essential for Biomass Remote Sensing Missions *Surveys in Geophysics* **40** 863–80 Online:
 560 <https://doi.org/10.1007/s10712-019-09528-w>
- 561 Collier N, Hoffman F M, Lawrence D M, Keppel-Aleks G, Koven C D, Riley W J, Mu M and Randerson J T
 562 2018 The International Land Model Benchmarking (ILAMB) System: Design, Theory, and Implementation
 563 *Journal of Advances in Modeling Earth Systems* **10** 2731–54 Online:
 564 <http://agupubs.onlinelibrary.wiley.com/doi/abs/10.1029/2018MS001354>
- 565 Cook-Patton S C, Leavitt S M, Gibbs D, Harris N L, Lister K, Anderson-Teixeira K J, Briggs R D, Chazdon
 566 R L, Crowther T W, Ellis P W, Griscom H P, Herrmann V, Holl K D, Houghton R A, Larrosa C, Lomax G,
 567 Lucas R, Madsen P, Malhi Y, Paquette A, Parker J D, Paul K, Routh D, Roxburgh S, Saatchi S, Hoogen J
 568 van den, Walker W S, Wheeler C E, Wood S A, Xu L and Griscom B W 2020 Mapping carbon accumulation
 569 potential from global natural forest regrowth *Nature* **585** 545–50 Online:
 570 <http://www.nature.com/articles/s41586-020-2686-x>
- 571 Curtis P G, Slay C M, Harris N L, Tyukavina A and Hansen M C 2018 Classifying drivers of global forest
 572 loss *Science* **361** 1108–11 Online: <http://science.sciencemag.org/content/361/6407/1108>
- 573 Curtis P S and Gough C M 2018 Forest aging, disturbance and the carbon cycle *New Phytologist* **219**
 574 1188–93 Online: <http://nph.onlinelibrary.wiley.com/doi/abs/10.1111/nph.15227>
- 575 Di Vittorio A V, Shi X, Bond-Lamberty B, Calvin K and Jones A 2020 Initial Land Use/Cover Distribution
 576 Substantially Affects Global Carbon and Local Temperature Projections in the Integrated Earth System
 577 Model *Global Biogeochemical Cycles* **34** Online:
 578 <https://onlinelibrary.wiley.com/doi/abs/10.1029/2019GB006383>
- 579 FAO 2010 *Global Forest Resources Assessment 2010* (Rome, Italy: Food; Agriculture Organization of the
 580 United Nations)
- 581 Friedlingstein P, Cox P, Betts R, Bopp L, Bloh W von, Brovkin V, Cadule P, Doney S, Eby M, Fung I, Bala
 582 G, John J, Jones C, Joos F, Kato T, Kawamiya M, Knorr W, Lindsay K, Matthews H D, Raddatz T, Rayner
 583 P, Reick C, Roeckner E, Schnitzler K-G, Schnur R, Strassmann K, Weaver A J, Yoshikawa C and Zeng N
 584 2006 Climate–Carbon Cycle Feedback Analysis: Results from the C4MIP Model Intercomparison *Journal of*
 585 *Climate* **19** 3337–53 Online: <https://journals.ametsoc.org/doi/abs/10.1175/JCLI3800.1>
- 586 Friedlingstein P, Jones M W, O’Sullivan M, Andrew R M, Hauck J, Peters G P, Peters W, Pongratz J, Sitch
 587 S, Le Quéré C, Bakker D C E, Canadell J G, Ciais P, Jackson R B, Anthoni P, Barbero L, Bastos A,
 588 Bastrikov V, Becker M, Bopp L, Buitenhuis E, Chandra N, Chevallier F, Chini L P, Currie K I, Feely R A,
 589 Gehlen M, Gilfillan D, Gkritzalis T, Goll D S, Gruber N, Gutekunst S, Harris I, Haverd V, Houghton R A,

- 590 Hurtt G, Ilyina T, Jain A K, Joetzjer E, Kaplan J O, Kato E, Klein Goldewijk K, Korsbakken J I,
 591 Landschützer P, Lauvset S K, Lefèvre N, Lenton A, Lienert S, Lombardozzi D, Marland G, McGuire P C,
 592 Melton J R, Metzl N, Munro D R, Nabel J E M S, Nakaoka S-I, Neill C, Omar A M, Ono T, Peregon A,
 593 Pierrot D, Poulter B, Rehder G, Resplandy L, Robertson E, Rödenbeck C, Séférian R, Schwinger J, Smith N,
 594 Tans P P, Tian H, Tilbrook B, Tubiello F N, Werf G R van der, Wiltshire A J and Zaehle S 2019 Global
 595 Carbon Budget 2019 *Earth System Science Data* **11** 1783–838 Online:
 596 <https://essd.copernicus.org/articles/11/1783/2019/>
- 597 Gillman L N, Wright S D, Cusens J, McBride P D, Malhi Y and Whittaker R J 2015 Latitude, productivity
 598 and species richness *Global Ecology and Biogeography* **24** 107–17 Online:
 599 <https://onlinelibrary.wiley.com/doi/abs/10.1111/geb.12245>
- 600 Goldstein A, Turner W R, Spawn S A, Anderson-Teixeira K J, Cook-Patton S, Fargione J, Gibbs H K,
 601 Griscom B, Hewson J H, Howard J F, Ledezma J C, Page S, Koh L P, Rockström J, Sanderman J and Hole
 602 D G 2020 Protecting irrecoverable carbon in Earth's ecosystems *Nature Climate Change* 1–9 Online:
 603 <http://www.nature.com/articles/s41558-020-0738-8>
- 604 Grassi G, House J, Dentener F, Federici S, Elzen M den and Penman J 2017 The key role of forests in
 605 meeting climate targets requires science for credible mitigation *Nature Climate Change* **7** 220–6 Online:
 606 <https://www.nature.com/articles/nclimate3227>
- 607 Griscom B W, Adams J, Ellis P W, Houghton R A, Lomax G, Miteva D A, Schlesinger W H, Shoch D,
 608 Siikamäki J V, Smith P, Woodbury P, Zganjar C, Blackman A, Campari J, Conant R T, Delgado C, Elias P,
 609 Gopalakrishna T, Hamsik M R, Herrero M, Kiesecker J, Landis E, Laestadius L, Leavitt S M, Minnemeyer S,
 610 Polasky S, Potapov P, Putz F E, Sanderman J, Silvius M, Wollenberg E and Fargione J 2017 Natural climate
 611 solutions *Proceedings of the National Academy of Sciences* **114** 11645–50 Online:
 612 <http://www.pnas.org/lookup/doi/10.1073/pnas.1710465114>
- 613 Gustafson E J, Kubiske M E, Miranda B R, Hoshika Y and Paoletti E 2018 Extrapolating plot-scale CO₂
 614 and ozone enrichment experimental results to novel conditions and scales using mechanistic modeling
 615 *Ecological Processes* **7** 31 Online: <https://doi.org/10.1186/s13717-018-0142-8>
- 616 Hansen M C, Potapov P V, Moore R, Hancher M, Turubanova S A, Tyukavina A, Thau D, Stehman S V,
 617 Goetz S J, Loveland T R, Kommareddy A, Egorov A, Chini L, Justice C O and Townshend J R G 2013
 618 High-Resolution Global Maps of 21st-Century Forest Cover Change *Science* **342** 850–3 Online:
 619 <http://www.sciencemag.org/cgi/doi/10.1126/science.1244693>
- 620 Harmon M E, Bond-Lamberty B, Tang J and Vargas R 2011 Heterotrophic respiration in disturbed forests:
 621 A review with examples from North America *Journal of Geophysical Research* **116** Online:
 622 <http://doi.wiley.com/10.1029/2010JG001495>
- 623 Houghton R A 2020 Terrestrial fluxes of carbon in GCP carbon budgets *Global Change Biology* **26** 3006–14
 624 Online: <https://onlinelibrary.wiley.com/doi/abs/10.1111/gcb.15050>
- 625 Hu T, Su Y, Xue B, Liu J, Zhao X, Fang J and Guo Q 2016 Mapping Global Forest Aboveground Biomass
 626 with Spaceborne LiDAR, Optical Imagery, and Forest Inventory Data *Remote Sensing* **8** 565 Online:
 627 <http://www.mdpi.com/2072-4292/8/7/565>
- 628 IPCC 2019 *2019 Refinement to the 2006 IPCC Guidelines for National Greenhouse Gas Inventories* Online:

- 629 <https://www.ipcc.ch/report/2019-refinement-to-the-2006-ipcc-guidelines-for-national-greenhouse-gas-inventories/>
- 630
- 631 IPCC 2018 *Global Warming of 1.5°C. An IPCC Special Report on the impacts of global warming of 1.5°C above pre-industrial levels and related global greenhouse gas emission pathways, in the context of strengthening the global response to the threat of climate change, sustainable development, and efforts to eradicate poverty* [Masson-Delmotte, V., P. Zhai, H.-O. Pörtner, D. Roberts, J. Skea, P.R. Shukla, A. Pirani, W. Moufouma-Okia, C. Péan, R. Pidcock, S. Connors, J.B.R. Matthews, Y. Chen, X. Zhou, M.I. Gomis, E. Lonnoy, T. Maycock, M. Tignor, and T. Waterfield (eds.)]. Online: <https://www.ipcc.ch/sr15/>
- 632
- 633
- 634
- 635
- 636
- 637 Jian J, Vargas R, Anderson-Teixeira K, Stell E, Herrmann V, Horn M, Kholod N, Manzon J, Marchesi R,
- 638 Paredes D and Bond-Lamberty B 2020 *A restructured and updated global soil respiration database*
- 639 (*SRDB-V5*) (Data, Algorithms,; Models) Online: <https://essd.copernicus.org/preprints/essd-2020-136/>
- 640 Johnson D J, Needham J, Xu C, Massoud E C, Davies S J, Anderson-Teixeira K J, Bunyavejchewin S,
- 641 Chambers J Q, Chang-Yang C-H, Chiang J-M, Chuyong G B, Condit R, Cordell S, Fletcher C, Giardina C P,
- 642 Giambelluca T W, Gunatilleke N, Gunatilleke S, Hsieh C-F, Hubbell S, Inman-Narahari F, Kassim A R,
- 643 Katabuchi M, Kenfack D, Litton C M, Lum S, Mohamad M, Nasardin M, Ong P S, Ostertag R, Sack L,
- 644 Swenson N G, Sun I F, Tan S, Thomas D W, Thompson J, Umaña M N, Uriarte M, Valencia R, Yap S,
- 645 Zimmerman J, McDowell N G and McMahon S M 2018 Climate sensitive size-dependent survival in tropical
- 646 trees *Nature Ecology & Evolution* **2** 1436–42 Online: <http://www.nature.com/articles/s41559-018-0626-z>
- 647 Jung M, Henkel K, Herold M and Churkina G 2006 Exploiting synergies of global land cover products for
- 648 carbon cycle modeling *Remote Sensing of Environment* **101** 534–53 Online:
- 649 <http://www.sciencedirect.com/science/article/pii/S0034425706000514>
- 650 Keith H, Mackey B G and Lindenmayer D B 2009 Re-evaluation of forest biomass carbon stocks and lessons
- 651 from the world's most carbon-dense forests *Proceedings of the National Academy of Sciences* **106** 11635–40
- 652 Online: <http://www.pnas.org/content/106/28/11635.abstract>
- 653 Konings A G, Bloom A A, Liu J, Parazoo N C, Schimel D S and Bowman K W 2019 Global satellite-driven
- 654 estimates of heterotrophic respiration *Biogeosciences* **16** 2269–84 Online:
- 655 <https://bg.copernicus.org/articles/16/2269/2019/>
- 656 Köchy M, Hiederer R and Freibauer A 2015 Global distribution of soil organic carbon – Part 1: Masses and
- 657 frequency distributions of SOC stocks for the tropics, permafrost regions, wetlands, and the world *SOIL* **1**
- 658 351–65 Online: <https://soil.copernicus.org/articles/1/351/2015/>
- 659 Krause A, Pugh T A M, Bayer A D, Li W, Leung F, Bondeau A, Doelman J C, Humpenöder F, Anthoni P,
- 660 Bodirsky B L, Ciais P, Müller C, Murray-Tortarolo G, Olin S, Popp A, Sitch S, Stehfest E and Arneth A
- 661 2018 Large uncertainty in carbon uptake potential of land-based climate-change mitigation efforts *Global*
- 662 *Change Biology* **24** 3025–38 Online: <https://onlinelibrary.wiley.com/doi/abs/10.1111/gcb.14144>
- 663 Li X and Xiao J 2019 Mapping Photosynthesis Solely from Solar-Induced Chlorophyll Fluorescence: A
- 664 Global, Fine-Resolution Dataset of Gross Primary Production Derived from OCO-2 *Remote Sensing* **11** 2563
- 665 Online: <https://www.mdpi.com/2072-4292/11/21/2563>
- 666 Lichstein J W, Wirth C, Horn H S and Pacala S W 2009 Biomass Chronosequences of United States Forests:
- 667 Implications for Carbon Storage and Forest Management *Old-Growth Forests Ecological Studies* ed C Wirth,

- 668 G Gleixner and M Heimann (Springer Berlin Heidelberg) pp 301–41 Online:
 669 http://link.springer.com/chapter/10.1007/978-3-540-92706-8_14
- 670 Liu J, Bowman K, Parazoo N C, Bloom A A, Wunch D, Jiang Z, Gurney K R and Schimel D 2018 Detecting
 671 drought impact on terrestrial biosphere carbon fluxes over contiguous US with satellite observations
 672 *Environmental Research Letters* **13** 095003 Online: <https://doi.org/10.1088%2F1748-9326%2Faad5ef>
- 673 Lutz J A, Furniss T J, Johnson D J, Davies S J, Allen D, Alonso A, Anderson-Teixeira K J, Andrade A,
 674 Baltzer J, Becker K M L, Blomdahl E M, Bourg N A, Bunyavejchewin S, Burslem D F R P, Cansler C A,
 675 Cao K, Cao M, Cárdenas D, Chang L-W, Chao K-J, Chao W-C, Chiang J-M, Chu C, Chuyong G B, Clay K,
 676 Condit R, Cordell S, Dattaraja H S, Duque A, Ewango C E N, Fischer G A, Fletcher C, Freund J A,
 677 Giardina C, Germain S J, Gilbert G S, Hao Z, Hart T, Hau B C H, He F, Hector A, Howe R W, Hsieh C-F,
 678 Hu Y-H, Hubbell S P, Inman-Narahari F M, Itoh A, Janík D, Kassim A R, Kenfack D, Korte L, Král K,
 679 Larson A J, Li Y, Lin Y, Liu S, Lum S, Ma K, Makana J-R, Malhi Y, McMahon S M, McShea W J,
 680 Memighe H R, Mi X, Morecroft M, Musili P M, Myers J A, Novotny V, Oliveira A de, Ong P, Orwig D A,
 681 Ostertag R, Parker G G, Patankar R, Phillips R P, Reynolds G, Sack L, Song G-Z M, Su S-H, Sukumar R,
 682 Sun I-F, Suresh H S, Swanson M E, Tan S, Thomas D W, Thompson J, Uriarte M, Valencia R, Vicentini A,
 683 Vrška T, Wang X, Weiblen G D, Wolf A, Wu S-H, Xu H, Yamakura T, Yap S and Zimmerman J K 2018
 684 Global importance of large-diameter trees *Global Ecology and Biogeography* **27** 849–64 Online:
 685 <https://onlinelibrary.wiley.com/doi/abs/10.1111/geb.12747>
- 686 Luyssaert S, Inglima I, Jung M, Richardson A D, Reichstein M, Papale D, Piao S L, Schulze E-D, Wingate L,
 687 Matteucci G, Aragao L, Aubinet M, Beer C, Bernhofer C, Black K G, Bonal D, Bonnefond J-M, Chambers J,
 688 Ciais P, Cook B, Davis K J, Dolman A J, Gielen B, Goulden M, Grace J, Granier A, Grelle A, Griffis T,
 689 Grünwald T, Guidolotti G, Hanson P J, Harding R, Hollinger D Y, Hutyra L R, Kolari P, Kruijt B, Kutsch
 690 W, Lagergren F, Laurila T, Law B E, Maire G L, Lindroth A, Loustau D, Malhi Y, Mateus J, Migliavacca M,
 691 Misson L, Montagnani L, Moncrieff J, Moors E, Munger J W, Nikinmaa E, Ollinger S V, Pita G, Rebmann
 692 C, Roupsard O, Saigusa N, Sanz M J, Seufert G, Sierra C, Smith M-L, Tang J, Valentini R, Vesala T and
 693 Janssens I A 2007 CO₂ balance of boreal, temperate, and tropical forests derived from a global database
 694 *Global Change Biology* **13** 2509–37 Online:
 695 <http://onlinelibrary.wiley.com/doi/abs/10.1111/j.1365-2486.2007.01439.x>
- 696 Luyssaert S, Schulze E D, Borner A, Knohl A, Hessenmoller D, Law B E, Ciais P and Grace J 2008
 697 Old-growth forests as global carbon sinks *Nature* **455** 213 Online:
 698 http://dx.doi.org/10.1038/nature07276%20http://www.nature.com/nature/journal/v455/n7210/supplinfo/nature07276_S1.html
- 700 Magnani F, Mencuccini M, Borghetti M, Berbigier P, Berninger F, Delzon S, Grelle A, Hari P, Jarvis P G,
 701 Kolari P, Kowalski A S, Lankreijer H, Law B E, Lindroth A, Loustau D, Manca G, Moncrieff J B, Rayment
 702 M, Tedeschi V, Valentini R and Grace J 2007 The human footprint in the carbon cycle of temperate and
 703 boreal forests *Nature* **447** 849–51 Online: <http://www.nature.com/articles/nature05847>
- 704 Maurer G E, Chan A M, Trahan N A, Moore D J P and Bowling D R 2016 Carbon isotopic composition of
 705 forest soil respiration in the decade following bark beetle and stem girdling disturbances in the Rocky
 706 Mountains *Plant, Cell & Environment* **39** 1513–23 Online:
 707 <http://onlinelibrary.wiley.com/doi/abs/10.1111/pce.12716>

- 708 McDowell N G, Allen C D, Anderson-Teixeira K, Aukema B H, Bond-Lamberty B, Chini L, Clark J S,
709 Dietze M, Grossiord C, Hanbury-Brown A, Hurt G C, Jackson R B, Johnson D J, Kueppers L, Lichstein J
710 W, Ogle K, Poulter B, Pugh T A M, Seidl R, Turner M G, Uriarte M, Walker A P and Xu C 2020 Pervasive
711 shifts in forest dynamics in a changing world *Science* **368** Online:
712 <https://science.sciencemag.org/content/368/6494/eaaz9463>
- 713 McDowell N G, Michaletz S T, Bennett K E, Solander K C, Xu C, Maxwell R M and Middleton R S 2018
714 Predicting Chronic Climate-Driven Disturbances and Their Mitigation *Trends in Ecology & Evolution* **33**
715 15–27 Online: [https://www.cell.com/trends/ecology-evolution/abstract/S0169-5347\(17\)30261-6](https://www.cell.com/trends/ecology-evolution/abstract/S0169-5347(17)30261-6)
- 716 McGarvey J C, Thompson J R, Epstein H E and Shugart H H 2014 Carbon storage in old-growth forests of
717 the Mid-Atlantic: Toward better understanding the eastern forest carbon sink *Ecology* **96** 311–7 Online:
718 <http://www.esajournals.org/doi/abs/10.1890/14-1154.1>
- 719 Novick K A, Biederman J A, Desai A R, Litvak M E, Moore D J P, Scott R L and Torn M S 2018 The
720 AmeriFlux network: A coalition of the willing *Agricultural and Forest Meteorology* **249** 444–56 Online:
721 <http://www.sciencedirect.com/science/article/pii/S0168192317303295>
- 722 Pan Y, Birdsey R A, Fang J, Houghton R, Kauppi P E, Kurz W A, Phillips O L, Shvidenko A, Lewis S L,
723 Canadell J G, Ciais P, Jackson R B, Pacala S, McGuire A D, Piao S, Rautiainen A, Sitch S and Hayes D
724 2011 A Large and Persistent Carbon Sink in the World's Forests *Science* **333** 988–93 Online:
725 <http://www.sciencemag.org/content/early/2011/07/27/science.1201609.abstract>
- 726 Phillips C L, Bond-Lamberty B, Desai A R, Lavoie M, Risk D, Tang J, Todd-Brown K and Vargas R 2017
727 The value of soil respiration measurements for interpreting and modeling terrestrial carbon cycling *Plant and*
728 *Soil* **413** 1–25 Online: <http://link.springer.com/10.1007/s11104-016-3084-x>
- 729 Pregitzer K S and Euskirchen E S 2004 Carbon cycling and storage in world forests: Biome patterns related
730 to forest age *Global Change Biology* **10** 2052–77 Online: <http://dx.doi.org/10.1111/j.1365-2486.2004.00866.x>
- 731 Pugh T A M, Lindeskog M, Smith B, Poulter B, Arneth A, Haverd V and Calle L 2019 Role of forest
732 regrowth in global carbon sink dynamics *Proceedings of the National Academy of Sciences* **116** 4382–7
733 Online: <http://www.pnas.org/lookup/doi/10.1073/pnas.1810512116>
- 734 R Core Team 2020 R: A language and environment for statistical computing. R Foundation for Statistical
735 Computing, Vienna, Austria. URL <http://www.R-project.org/>.
- 736 Requena Suarez D, Rozendaal D M A, Sy V D, Phillips O L, Alvarez-Dávila E, Anderson-Teixeira K,
737 Araujo-Murakami A, Arroyo L, Baker T R, Bongers F, Brienen R J W, Carter S, Cook-Patton S C,
738 Feldpausch T R, Griscom B W, Harris N, Héault B, Coronado E N H, Leavitt S M, Lewis S L, Marimon B
739 S, Mendoza A M, N'dja J K, N'Guessan A E, Poorter L, Qie L, Rutishauser E, Sist P, Sonké B, Sullivan M J
740 P, Vilanova E, Wang M M H, Martius C and Herold M 2019 Estimating aboveground net biomass change for
741 tropical and subtropical forests: Refinement of IPCC default rates using forest plot data *Global Change
742 Biology* **25** 3609–24 Online: <http://onlinelibrary.wiley.com/doi/abs/10.1111/gcb.14767>
- 743 Ribeiro-Kumara C, Köster E, Aaltonen H and Köster K 2020 How do forest fires affect soil greenhouse gas
744 emissions in upland boreal forests? A review *Environmental Research* **184** 109328 Online:
745 <http://www.sciencedirect.com/science/article/pii/S0013935120302218>
- 746 Saatchi S S, Harris N L, Brown S, Lefsky M, Mitchard E T A, Salas W, Zutta B R, Buermann W, Lewis S L,

- 747 Hagen S, Petrova S, White L, Silman M and Morel A 2011 Benchmark map of forest carbon stocks in
 748 tropical regions across three continents *Proceedings of the National Academy of Sciences* **108** 9899–904
 749 Online: <http://www.pnas.org/content/108/24/9899>
- 750 Schepaschenko D, Chave J, Phillips O L, Lewis S L, Davies S J, Réjou-Méchain M, Sist P, Scipal K, Perger
 751 C, Herault B, Labrière N, Hofhansl F, Affum-Baffoe K, Aleinikov A, Alonso A, Amani C, Araujo-Murakami
 752 A, Armston J, Arroyo L, Ascarrunz N, Azevedo C, Baker T, Balazy R, Bedeau C, Berry N, Bilous A M,
 753 Bilous S Y, Bissiengou P, Blanc L, Bobkova K S, Braslavskaya T, Brienen R, Burslem D F R P, Condit R,
 754 Cuni-Sanchez A, Danilina D, Torres D del C, Derroire G, Descroix L, Sotta E D, d’Oliveira M V N, Dresel C,
 755 Erwin T, Evdokimenko M D, Falck J, Feldpausch T R, Foli E G, Foster R, Fritz S, Garcia-Abril A D,
 756 Gornov A, Gornova M, Gothard-Bassébé E, Gourlet-Fleury S, Guedes M, Hamer K C, Susanty F H, Higuchi
 757 N, Coronado E N H, Hubau W, Hubbell S, Ilstedt U, Ivanov V V, Kanashiro M, Karlsson A, Karminov V N,
 758 Killeen T, Koffi J-C K, Konovalova M, Kraxner F, Krejza J, Krisnawati H, Krivobokov L V, Kuznetsov M A,
 759 Lakyda I, Lakyda P I, Licona J C, Lucas R M, Lukina N, Lussetti D, Malhi Y, Manzanera J A, Marimon B,
 760 Junior B H M, Martinez R V, Martynenko O V, Matsala M, Matyashuk R K, Mazzei L, Memiaghe H,
 761 Mendoza C, Mendoza A M, Morozuk O V, Mukhortova L, Musa S, Nazimova D I, Okuda T, Oliveira L C,
 762 et al 2019 The Forest Observation System, building a global reference dataset for remote sensing of forest
 763 biomass *Scientific Data* **6** 1–11 Online: <http://www.nature.com/articles/s41597-019-0196-1>
- 764 Schimel D, Hargrove W, Hoffman F and MacMahon J 2007 NEON: A hierarchically designed national
 765 ecological network *Frontiers in Ecology and the Environment* **5** 59–9 Online:
 766 <http://esajournals.onlinelibrary.wiley.com/doi/abs/10.1890/1540-9295%282007%295%5B59%3ANAHDNE%5D2.0.CO%3B2>
- 768 Schimel D, Stephens B B and Fisher J B 2015 Effect of increasing CO₂ on the terrestrial carbon cycle
 769 *Proceedings of the National Academy of Sciences* **112** 436–41 Online:
 770 <http://www.pnas.org/lookup/doi/10.1073/pnas.1407302112>
- 771 Smithwick E A H, Harmon M E, Remillard S M, Acker S A and Franklin J F 2002 Potential upper bounds of
 772 carbon stores in forests of the Pacific Northwest *Ecological Applications* **12** 1303–17 Online:
 773 [http://doi.wiley.com/10.1890/1051-0761\(2002\)012%5B1303:PUBOCS%5D2.0.CO;2](http://doi.wiley.com/10.1890/1051-0761(2002)012%5B1303:PUBOCS%5D2.0.CO;2)
- 774 Song J, Wan S, Piao S, Knapp A K, Classen A T, Vicca S, Ciais P, Hovenden M J, Leuzinger S, Beier C,
 775 Kardol P, Xia J, Liu Q, Ru J, Zhou Z, Luo Y, Guo D, Adam Langley J, Zscheischler J, Dukes J S, Tang J,
 776 Chen J, Hofmockel K S, Kueppers L M, Rustad L, Liu L, Smith M D, Templer P H, Quinn Thomas R,
 777 Norby R J, Phillips R P, Niu S, Fatichi S, Wang Y, Shao P, Han H, Wang D, Lei L, Wang J, Li X, Zhang Q,
 778 Li X, Su F, Liu B, Yang F, Ma G, Li G, Liu Y, Liu Y, Yang Z, Zhang K, Miao Y, Hu M, Yan C, Zhang A,
 779 Zhong M, Hui Y, Li Y and Zheng M 2019 A meta-analysis of 1,119 manipulative experiments on terrestrial
 780 carbon-cycling responses to global change *Nature Ecology & Evolution* **3** 1309–20 Online:
 781 <http://www.nature.com/articles/s41559-019-0958-3>
- 782 Song X-P, Hansen M C, Stehman S V, Potapov P V, Tyukavina A, Vermote E F and Townshend J R 2018
 783 Global land change from 1982 to 2016 *Nature* **560** 639–43 Online:
 784 <http://www.nature.com/articles/s41586-018-0411-9/>
- 785 Spawn S A, Sullivan C C, Lark T J and Gibbs H K 2020 Harmonized global maps of above and belowground
 786 biomass carbon density in the year 2010 *Scientific Data* **7** 112 Online:

- 787 <http://www.nature.com/articles/s41597-020-0444-4>
- 788 Stoy P C, Mauder M, Foken T, Marcolla B, Boegh E, Ibrom A, Arain M A, Arneth A, Aurela M, Bernhofer
789 C, Cescatti A, Dellwik E, Duce P, Ganelle D, Gorsel E van, Kiely G, Knohl A, Margolis H, McCaughey H,
790 Merbold L, Montagnani L, Papale D, Reichstein M, Saunders M, Serrano-Ortiz P, Sottocornola M, Spano D,
791 Vaccari F and Varlagin A 2013 A data-driven analysis of energy balance closure across FLUXNET research
792 sites: The role of landscape scale heterogeneity *Agricultural and Forest Meteorology* **171-172** 137–52 Online:
793 <https://linkinghub.elsevier.com/retrieve/pii/S0168192312003413>
- 794 Sulman B N, Moore J A M, Abramoff R, Averill C, Kivlin S, Georgiou K, Sridhar B, Hartman M D, Wang
795 G, Wieder W R, Bradford M A, Luo Y, Mayes M A, Morrison E, Riley W J, Salazar A, Schimel J P, Tang J
796 and Classen A T 2018 Multiple models and experiments underscore large uncertainty in soil carbon dynamics
797 *Biogeochemistry* **141** 109–23 Online: <https://doi.org/10.1007/s10533-018-0509-z>
- 798 Taylor P G, Cleveland C C, Wieder W R, Sullivan B W, Doughty C E, Dobrowski S Z and Townsend A R
799 2017 Temperature and rainfall interact to control carbon cycling in tropical forests ed L Liu *Ecology Letters*
800 **20** 779–88 Online: <http://doi.wiley.com/10.1111/ele.12765>
- 801 Tubiello F N, Pekkarinen A, Marklund L, Wanner N, Conchedda G, Federici S, Rossi S and Grassi G 2020
802 Carbon Emissions and Removals by Forests: New Estimates 1990–2020 *Earth System Science Data
Discussions* 1–21 Online: <https://essd.copernicus.org/preprints/essd-2020-203/>
- 803 Vargas R, Allen M F and Allen E B 2008 Biomass and carbon accumulation in a fire chronosequence of a
804 seasonally dry tropical forest *Global Change Biology* **14** 109–24 Online:
805 <http://onlinelibrary.wiley.com/doi/abs/10.1111/j.1365-2486.2007.01462.x>
- 806 Wang Y, Ciais P, Goll D, Huang Y, Luo Y, Wang Y-P, Bloom A A, Broquet G, Hartmann J, Peng S,
807 Penuelas J, Piao S, Sardans J, Stocker B D, Wang R, Zaehle S and Zechmeister-Boltenstern S 2018
808 GOLUM-CNP v1.0: A data-driven modeling of carbon, nitrogen and phosphorus cycles in major terrestrial
809 biomes *Geoscientific Model Development* **11** 3903–28 Online:
810 <https://gmd.copernicus.org/articles/11/3903/2018/>
- 811 Warner D L, Bond-Lamberty B, Jian J, Stell E and Vargas R 2019 Spatial Predictions and Associated
812 Uncertainty of Annual Soil Respiration at the Global Scale *Global Biogeochemical Cycles* **33** 1733–45 Online:
813 <https://onlinelibrary.wiley.com/doi/abs/10.1029/2019GB006264>
- 814 Werf G R van der, Randerson J T, Giglio L, Leeuwen T T van, Chen Y, Rogers B M, Mu M, Marle M J E
815 van, Morton D C, Collatz G J, Yokelson R J and Kasibhatla P S 2017 Global fire emissions estimates during
816 1997–2016 *Earth System Science Data* **9** 697–720 Online: <https://essd.copernicus.org/articles/9/697/2017/>
- 817 Williams C A, Collatz G J, Masek J, Huang C and Goward S N 2014 Impacts of disturbance history on
818 forest carbon stocks and fluxes: Merging satellite disturbance mapping with forest inventory data in a carbon
819 cycle model framework *Remote Sensing of Environment* **151** 57–71 Online:
820 <https://linkinghub.elsevier.com/retrieve/pii/S0034425713004185>
- 821 Wilson R M, Hopple A M, Tfaily M M, Sebestyen S D, Schadt C W, Pfeifer-Meister L, Medvedeff C,
822 McFarlane K J, Kostka J E, Kolton M, Kolka R K, Kluber L A, Keller J K, Guilderson T P, Griffiths N A,
823 Chanton J P, Bridgman S D and Hanson P J 2016 Stability of peatland carbon to rising temperatures *Nature
Communications* **7** 13723 Online: <http://www.nature.com/articles/ncomms13723>

⁸²⁶ Xu M and Shang H 2016 Contribution of soil respiration to the global carbon equation *Journal of Plant
827 Physiology* **203** 16–28 Online: <https://linkinghub.elsevier.com/retrieve/pii/S0176161716301742>

⁸²⁸ Yang Y, Luo Y and Finzi A C 2011 Carbon and nitrogen dynamics during forest stand development: A
⁸²⁹ global synthesis *New Phytologist* **190** 977 Online: <http://dx.doi.org/10.1111/j.1469-8137.2011.03645.x>